

**UTILIZATION OF TEXTILE WASTE IN THE
MANUFACTURING OF PAVING BLOCKS
APPLICABLE FOR OUTDOOR SPORTS SURFACES**

Gannoru Kankanamalage Bhagya Maheshi Gannoruwa

(178074G)

Degree of Master of Science

Department of Civil Engineering

University of Moratuwa

Sri Lanka

May 2021

**UTILIZATION OF TEXTILE WASTE IN THE
MANUFACTURING OF PAVING BLOCKS
APPLICABLE FOR OUTDOOR SPORTS SURFACES**

Gannoru Kankanamalage Bhagya Maheshi Gannoruwa

(178074G)

Thesis submitted in partial fulfillment of the requirements for the degree
Master of Science in Civil Engineering

Department of Civil Engineering

University of Moratuwa

Sri Lanka

May 2021

DECLARATION

I declare that this is my own work and this thesis does not incorporate without acknowledgement any material previously submitted for a Degree or Diploma in any other University or Institute of higher learning and to the best of my knowledge and belief it does not contain any material previously published or written by another person except where the acknowledgement is made in the text.

Also, I hereby grant to the University of Moratuwa the non-exclusive right to reproduce and distribute my thesis in whole or in part in print, electronic or other medium. I retain the right to use this content in whole or in part in the future work (such as articles or books).

Signature:



Date: 06.05.2021

The above candidate has carried out research for the Master's thesis under my supervision.

Name of the Supervisor: Prof. S.M.A. Nanayakkara

Signature of the supervisor:

Date:

ABSTRACT

Synthetic fiber blended textile (polyester spandex) offcuts generated from apparel industry is considered as a waste; currently it is incinerated as fuel in the cement manufacturing process and remainder ends up in illegal dumps. In this study, use of textile waste especially polyester spandex as a raw material in building products was studied to help the apparel industry to manage textile waste in environmental friendly manner.

Accordingly, this research was focused on developing fabric embedded paving blocks applicable for foot paths and outdoor sports surfaces with improved shock absorption and water permeable characteristics.

In this study, optimum shredded fabric size and content was determined by testing cement paste specimens with shredded fabric for flexural and compressive strength. It was found that the shredded fabric pieces up to 10 mm in size enhanced the flexural and compressive strength due to reinforcing effect of fibers in the cement matrix and the optimum volume of fibers found to be about 26%. During the casting process of fabric-cement composites, it was found that use a viscosity modifying admixture helped to prevent segregation of fabric pieces. Furthermore a superplasticizer was used to improve the workability of mixes with low water/cement ratios. Paving blocks were produced with crushed rock fines as the filler material in fabric-cement composites.

Cast paving blocks with different mix proportions were tested for compressive strength, tensile splitting strength, abrasion resistance, skid resistance, water permeability, shock absorption capability and durability to evaluate its performance with requirements specified in SLS 1425, BSEN 1338 and BSEN 15330-1 to select the most suitable mixture. Based on test results, the optimum mix proportion was found to be: 26% of fabric, 25% of fine aggregate and 49% of cement by volume at 0.6 water/cement ratio with 0.3% of viscosity modifying agent (Mecellose) and 0.6% of superplasticizer (Hypercrete) by weight of cement.

Polyester spandex fabric embedded paving blocks complied with the requirements specified in BSEN 1338: 2003, (Concrete paving blocks- Requirements and test methods) As additional features, the developed paving block has the ability to reduce impact force by 20% which satisfying the requirement for outdoor sports surfaces for better foot comfort. Therefore, fabric embedded paving blocks can be recommended for outdoor sports surfaces. Furthermore, water infiltration capability of developed fabric embedded paving blocks is 100 times higher than that of conventional concrete paving blocks that can significantly lower the surface runoff during heavy rains.

ACKNOWLEDGEMENT

I wish to express special thank and sincere gratitude to my supervisor Prof. S.M.A. Nanayakkara, Professor of Civil Engineering at the Department of Civil Engineering, Faculty of Engineering, University of Moratuwa for his invaluable guidance, encouragements, patience and precious time that offered to me. I would like to thank the progress review committee, Prof. W.P.S. Dias and Prof. A.A.D.A.J. Perera for reviewing the research as well for the support given throughout the study.

I greatly appreciate and express my sincere gratitude to the Eng. (Dr). Asiri Karunawardena, Director General, National Building Research Organization (NBRO), Sri Lanka and the management staff of NBRO for granting funds and facilitating research needs.

I would like to extend my sincere gratitude and appreciation to the Departments of Civil Engineering and Materials Science and Engineering, University of Moratuwa, Sri Lanka and Building Materials Research and Testing Division, NBRO, Sri Lanka for providing the facilities to carry out the testing.

I would like to thank my family and my loved ones, who have supported me throughout the entire process. My warm hearted thanks to my friends Lumbini Ramasinghe and Madushani Ariyadasa for their endless support and encouragement to achieve this goal.

Gannoruwa G.K.B.M.

TABLE OF CONTENTS

LIST OF FIGURES	vi
LIST OF TABLES	viii
LIST OF ABBREVIATIONS	ix
CHAPTER 01	1
1 INTRODUCTION	1
1.1 Background	1
1.2 Objectives	3
CHAPTER 02	4
2 LITERATURE REVIEW	4
2.1 Polyester.....	4
2.2 Spandex.....	4
2.3 Polyester spandex	5
2.4 Previous research work on fabric embedded cement-based building products.....	6
CHAPTER 03	11
3 EXPERIMENTAL INVESTIGATION	11
3.1 Materials	11
3.2 Casting of tile samples	13
3.3 Casting and testing of cement paste prisms	15
3.3.1 Casting procedure.....	15
3.3.2 Flexural strength.....	18
3.3.3 Compressive strength	18
3.4 Casting and testing of paving blocks	18
3.4.1 Casting procedure.....	18
3.4.2 Compressive strength	20
3.4.3 Tensile splitting strength	21
3.4.4 Abrasion resistance	23
3.4.5 Skid resistance.....	24
3.4.6 Permeability	24

3.4.7	Shock absorption	26
3.4.8	Durability	32
3.4.8.1	Durability under moist and temperature conditions	32
CHAPTER 04	34
4	RESULTS AND DISCUSSION	34
4.1	The size distribution of fabric pieces	34
4.2	Particle size distribution of sand.....	37
4.3	Fiber composition of polyester spandex fabric.....	38
4.4	Weight per unit area of polyester spandex fabric	38
4.5	Particle density	39
4.6	Dispersion of fabric pieces in the cement matrix	39
4.7	Selection of suitable admixtures.....	42
4.8	Flexural and compressive strength of cement paste prisms.....	43
4.9	Failure pattern of fabric cement composites	48
4.10	Surface texture of fabric embedded paving blocks	49
4.11	Compressive strength of paving blocks	51
4.12	Tensile splitting strength.....	54
4.13	Abrasion resistance.....	59
4.14	Skid resistance.....	60
4.15	Permeability.....	61
4.16	Shock absorption	62
4.17	Durability.....	64
4.17.1	Durability under moist and temperature conditions	64
4.18	Cost calculation for fabric embedded paving block.....	65
5	CONCLUSIONS.....	67
References	69

LIST OF FIGURES

Figure 2.1: Structure of polyester	4
Figure 2.2: Chemical structure of spandex	5
Figure 2.3: Special features of spandex structure	5
Figure 2.4: Split section of waste cloth concrete [9].....	8
Figure 2.5: Surface appearance of fabric incorporated cement block [10]	8
Figure 2.6: The wool filaments used as fiber-reinforcement: (a) non-treated wool; (b) treated wool [12].....	9
Figure 3.1: Shredded form of fabric pieces	11
Figure 3.2: Steps used for casting of tile samples.....	14
Figure 3.3: Casting procedure of cement paste prism samples.....	16
Figure 3.4: Cone penetrometer	19
Figure 3.5: Casting procedure of paving blocks	20
Figure 3.6: Compression test of paving block	21
Figure 3.7: Splitting section of the test specimen	21
Figure 3.8: Tensile splitting test of paving block	22
Figure 3.9: Wide wheel abrasion tester.....	23
Figure 3.10: Pendulum friction test equipment.....	24
Figure 3.11: Cylindrical shape test specimen	25
Figure 3.12: Constant head permeameter	26
Figure 3.13: Designed shock absorption test apparatus	27
Figure 3.14: Load deformation variation of spring.....	28
Figure 3.15: Fabricated Artificial Athlete Apparatus	28
Figure 3.16: Moving system of artificial athlete apparatus	30
Figure 4.1: Size distribution of shredded fabric pieces.....	35
Figure 4.2: Image used for surface area analysis of fabric pieces	36
Figure 4.3: Area of analyzed fabric pieces belonged to different size segments	36
Figure 4.4: Particle size distribution of manufactured sand.....	38
Figure 4.5: Surface texture of fabric cement composite	40
Figure 4.6: Surface texture of tile samples belonged to different mix proportions	40
Figure 4.7: Surface texture of prism samples	41
Figure 4.8: Variations in the dispersion of fabric pieces in prism samples	43

Figure 4.9: Flexural strength variation with fabric content	44
Figure 4.10: Compressive strength variation with fabric content.....	45
Figure 4.11: Flexural strength variation with size of fabric pieces.....	47
Figure 4.12: Compressive strength variation with size of fabric pieces	47
Figure 4.13: Failure pattern under flexural load	48
Figure 4.14: Fracture surface under flexural load.....	49
Figure 4.15: Failure pattern under compression load	49
Figure 4.16: Surface texture of paving blocks belonged to different mix proportions	50
Figure 4.17: Load deformation pattern of paving block under compression load	51
Figure 4.18: Deformation of paving block	52
Figure 4.19: Failure pattern of paving block under compression test.....	52
Figure 4.20: Compressive strength variation of paving blocks	54
Figure 4.21: Loading arrangement of tensile splitting strength test	55
Figure 4.22: Tensile splitting strength variation of paving blocks	56
Figure 4.23: Failure pattern of paving block under tensile splitting test	57
Figure 4.24: Strength variation of selected paving block mixtures	58
Figure 4.25: Specimen subjected to the abrasion resistance test	59
Figure 4.26: Variation of water permeability in different mixtures.....	61
Figure 4.27: Use of force reduction capability to the benefit of athletes [32]	64
Figure 4.28: Dimensions of paving block.....	65

LIST OF TABLES

Table 2.1: Strength variations of fabric-cement composites with respect to fabric content [7]6	
Table 3.1: Mix proportions used for casting fabric incorporated tile specimens	14
Table 3.2: Mix proportions used for selection of suitable admixtures.....	17
Table 3.3: Mix proportions used for selection of suitable fabric incorporation.....	17
Table 3.4: Mix proportions used for selection of suitable sizes of fabric pieces	17
Table 4.1: Sieve analysis test results of fabric pieces	34
Table 4.2: Results of surface area analysis	37
Table 4.3: Sieve analysis test results of manufactured sand	37
Table 4.4: Change in water demand with fabric content	39
Table 4.5: Flexural and compressive strength values of prisms cast by changing fabric incorporation.....	44
Table 4.6: Flexural and compressive strength results of prisms cast with different sizes of fabrics.....	46
Table 4.7: Mix proportions used for casting of paving blocks	50
Table 4.8: Compressive strength results of fabric embedded paving blocks	53
Table 4.9: Tensile splitting strength of fabric embedded paving blocks	55
Table 4.10: Selected mix proportions for the casting of paving blocks.....	57
Table 4.11: Strength results of selected paving block mixtures	58
Table 4.12: Abrasion resistance test results	59
Table 4.13: Skid resistance test results	60
Table 4.14: Permeability test results.....	61
Table 4.15: Shock absorption test results	63
Table 4.16: Durability evaluation results under moist and temperature conditions	64
Table 4.17: Material cost for fabric embedded paving block	66

LIST OF ABBREVIATIONS

AAA	Artificial Athlete Apparatus
ABC	Aggregate Base Course
C	Cellulose based viscosity modifier
FV	Fabric content by volume
GDP	Gross Domestic Product
GSM	Grams per square meter
H	Poly-carboxylic ether based superplasticizer
MS	Manufactured Sand
USRV	Unpolished Slip Resistance Value
W/C	Water: Cement ratio

CHAPTER 01

1 INTRODUCTION

1.1 Background

In Sri Lanka, the apparel industry is the most significant and dynamic contributor to the economy. In 2015, the apparel industry contributed to 61% of exports and 44% of GDP while focusing on sustainable manufacturing processes [1]. However, there are no well-established textile waste recycling facilities in Sri Lanka. Therefore, in the past, substantial amount of waste had been used to export nearby countries where textile recycling facilities exist. It became an inconvenient solution due to the high export cost and anti-dumping regulations established in China and Malaysia since 2007. Some of the synthetic waste is being sent to cement kilns where it is incinerated as fuel in the cement manufacturing process. The ever increasing amount of synthetic waste exceeds the burning capacity of cement kilns. Consequently, in Sri Lanka, a part of textile waste ends up in illegal dumps or else, burnt thus increasing environmental pollution.

Post-production textile waste can be categorized into different types as follows.

Excessive rolls – that are less problematic

Rejected fabric – branded fabrics that are destroyed for brand protection and the non-branded fabrics that are sold at a bargain price.

Rejected products - faulty product rate is kept less than 1%.

Offcuts – 15% to 18% of the total used fabrics are left as offcuts. Cotton offcuts can be recycled as cotton yarn but offcuts generated from synthetic blended fabrics are usually unrecyclable. Spandex mixed offcuts (e.g. Polyester Spandex) are difficult to recycle, therefore apparel industry pays a high price to incinerate them at cement kilns including transportation and burning costs. Other than that, local small scale businesses use cotton offcuts to weave mats and carpets. Synthetic fiber blended offcuts are the most problematic waste.

In the apparel industry, fabric offcuts is the biggest waste in volume. Sri Lankan apparel industry generates fabric offcuts approximately 44,100 tons per year [1]. The use of synthetic blended fabric is approximately 40% of total fabric usage and those offcuts create a significant waste disposal problem. Accordingly, synthetic fiber blended fabric offcut generation is approximately 17,640 tons per year. Utilization of this waste as a raw material for other industries is the best way to lessen the fabric waste disposal issue. The use of waste materials in the construction sector has been a promising area, primarily aiming to protect the environment from illegal dumping.

In the apparel industry, polyester spandex fabric is mainly used for body-conforming garments such as sportswear. Polyester spandex is a synthetic fiber blended fabric with superior elasticity, woven using polyester fibers and spandex fibers [2]. Fiber composition depends on the desirable properties of the fabric, polyester fiber content varies from 60-95% while spandex fiber content varies from 40-5% [3] and Eng. Dhanujie Jayapala was given the data during a phone conversation (Manager-Environmental sustainability, MAS Capital Pvt Ltd, personal communication, November 28, 2018). Polyester spandex is a material difficult to recycle because of its spandex blend and its offcuts are considered as waste. Therefore in this research, polyester spandex waste was considered in developing cement-based paving blocks.

Pavement structures can be categorized into two types, such as flexible pavements and rigid pavements, based on its load distribution. Normal concrete based pavements are considered as rigid pavements and asphalt pavements are considered as flexible pavements. Accordingly, flexible pavements are more comfortable for travelling than rigid pavements.

Flexible pavements are most suitable for footpaths, jogging tracks and outdoor sports surfaces due to its ability to facilitate better foot comfort for users. As the current practice in Sri Lanka, normal concrete paving blocks are used for footpaths and jogging tracks, but the hardness of these surfaces may give rise to health issues by affecting in knee joints and ankle joints of its users.

This study seeks the possibility of utilizing synthetic fiber blended fabric offcuts such as polyester spandex as a reinforcing filler in the development of fabric-cement

composites applicable to pavement structures with improved permeable and shock absorption characteristics.

1.2 Objective

Development of paving blocks with better walking comfort characteristics by embedding fabric wastes containing spandex while satisfying relevant industrial standards.

CHAPTER 02

2 LITERATURE REVIEW

2.1 Polyester

Polyester is a type of polymer that contains an ester functional group in the main chain and it is the product of polymerization between dicarboxylic acid and diol with the elimination of water. The chemical structure of polyester is given in Figure 2.1. Polyester fibers are sometimes spun together with natural or synthetic fibers to produce a cloth with blended properties. Polyester thread or yarn is commonly used in the apparel industry. Polyester fabrics shows a low water absorption property [4].

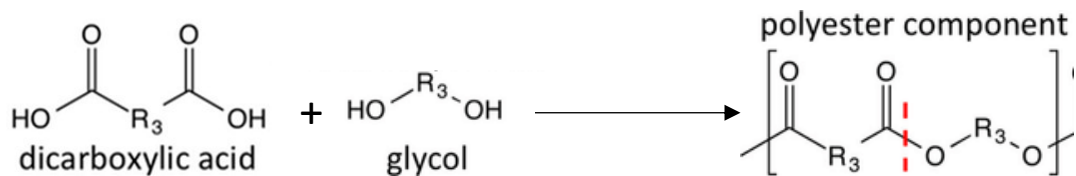


Figure 2.1: Structure of polyester

Polyester fiber's structure is a combination of crystalline and noncrystalline regions. The chemical structure of polyester is unsaturated due to the presence of double bonds in the backbone which may affect the UV stability of the polymer.

2.2 Spandex

Spandex is a synthetic fiber best known for its exceptional elasticity [5]. It is stronger and more durable than natural rubber. Spandex has been incorporated into a wide range of garments, especially in skin-tight garments due to its elasticity and strength. Benefits of spandex are its significant strength and elasticity and its ability to return to the original shape after stretching and faster drying than ordinary fabrics. For clothing, spandex is usually mixed with cotton or polyester and accounts for a small percentage of the final fabric, which therefore retains most of the look and feel of the other fibers.

Spandex is scientifically called lycra and it allows the fiber to stretch up to 600% without any permanent deformation [5]. The spandex fiber backbone consists of

flexible macro glycol and stiff di-isocyanate. The chemical structure of spandex is given in Figure 2.2.

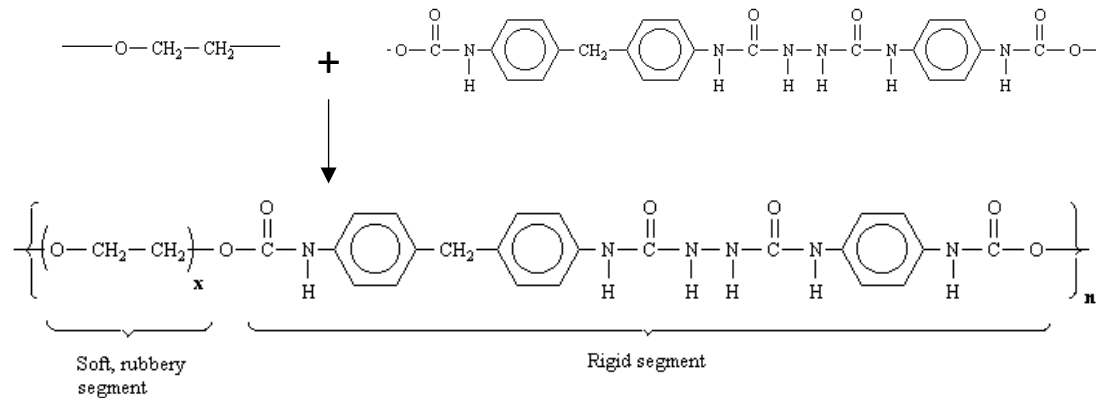


Figure 2.2: Chemical structure of spandex

The elasticity of spandex is a direct result of the material's chemical composition which consists of a flexible (amorphous) segment and rigid segment as shown in Figure 2.3. When a tensile force is applied to the spandex fiber, interactive bonds between rigid segments are broken while giving the straightening out capability to amorphous segments. Thereby, fiber length is increased due to longer amorphous segments. When fiber is straightening out to its maximum length, interactive bonds are formed between rigid segments while making the fiber stiffer and stronger. After the removal of the tensional force, amorphous segments recoil while returning the fiber to its relaxed state [6].

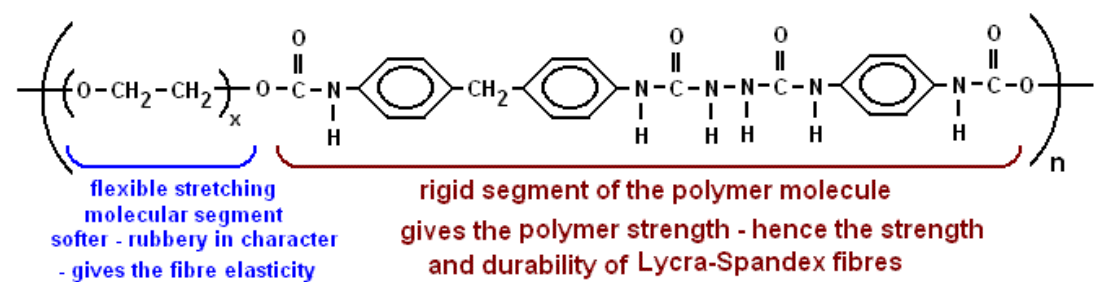


Figure 2.3: Special features of spandex structure

2.3 Polyester spandex

Fabric blend is a combination of two or more different types of fibers together to create a fabric with unique properties. Polyester is often blended with spandex to achieve

superior elastic and comfort characteristics to produce sports clothes, swimwear, and body- confirming garments. Fiber composition may vary depending on the desired properties of the woven fabric. Depending on the application, polyester content varies from 95-60% and spandex content varies from 5-40% in the polyester spandex fabric.

Polyester spandex is difficult to recycle due to its spandex blend, therefore currently rejected fabrics and offcuts are disposed as waste.

2.4 Previous research work on fabric embedded cement-based building products

Aspiras et al. [7], utilized textile waste cuttings as building materials, producing a composite material from a mixture of textile waste cuttings, cement and water. Textile cuttings had average lengths of 2cm and 6cm, and mixed with Portland cement binder in textile waste-cement ratios of 1:3, 1:4, and 1:5 by weight. Water was added in amounts corresponding to water-cement ratios ranging from 0.53 to 0.85. The samples tested for compression did not exhibit a sudden brittle fracture even beyond the failure load, indicating its high energy-absorbing capacity. The test results are summarized in Table 2.1.

The incorporation of fabric pieces leads to an increase in the flexural properties of the composite which demonstrates the reinforcing behavior of fabric pieces in the cement matrix.

Table 2.1: Strength variations of fabric-cement composites with respect to fabric content [7]

Design Mix	W/C	Long Fibers (6cm)				Short Fibers (2cm)			
Fiber: Cement		Water Absorption (%)	Strength (MPa)			Water Absorption (%)	Strength (MPa)		
			Compressive	Tensile	Flexural		Compressive	Tensile	Flexural
1 : 3	0.75	41.638	4.918	4.199	8.186	43.728	4.781	3.936	7.921
1 : 4	0.63	28.295	7.286	7.821	11.780	28.533	7.227	7.406	11.576
1 : 5	0.53	23.925	8.482	9.243	16.138	24.094	8.430	8.885	16.020

In spite of the high flammability of the textile waste cuttings, the composite material showed no evidence of burning when subjected to open flame for 30 minutes. The result of the laboratory test indicated a sturdy lighter-than-concrete building material. The fabric incorporated cement paste specimens look like concrete but lighter in weight and it can be cut or nailed like wood. The fabric-cement composite has potential uses for ceilings, walls, wooden board substitute, or as an economical alternative concrete block [7].

Kulathunga et al. [8] experimented using fabric waste as a reinforcing agent to cast flat tiles with cement: fabric waste: sand ratios of 1:1:3 and 1:2:3. A pressing mechanism was used to cast tiles. The thicknesses of two tile samples were 25mm and 13mm. Flexural strength, water absorption and density were measured as per SLS 863: [Specification for Cement Concrete Tiles], which covers requirements for cement concrete for floor tiles and wall tiles. The transverse strengths for the two mixed proportions were 1.7 MPa and 2.51 MPa respectively, water absorptions were 4.7% and 6.2%.

Selvaraj et al. [9] studied on recycled waste cloth in concrete. Synthetic and semi-synthetic fabric pieces of 20 mm x 20 mm size were incorporated to cement, sand and coarse aggregate mixture as 1-5% by weight of cement. w/c ratio was increased with the increment of fabric content. Fabric cuttings contribute to increasing the volume of the mixture but it may not be conceived as either an aggregate or reinforcement. The compressive strength of the concrete gradually reduced with the increment of the percentage of incorporated fabric materials. Strength reduced due to the reduction of cohesiveness in the concrete matrix. It is due to the formation of calcium silicate hydrate is not fully around the fine or coarse aggregate and it is partially formed on the waste fabric. Flexural strength and impact energy absorption of concrete increased with the increment of fabric content. Tensile splitting strength of the concrete increased up to 4% addition of fabric pieces by weight of cement and thereafter it was reduced when compared with control mixture of concrete. This concrete has a high affinity to water, therefore it is better to use with special waterproof coating. Cross-section of waste cloth concrete is shown in Figure 2.4.



Figure 2.4: Split section of waste cloth concrete [9]

Basnayake et al. [10] cast cement blocks by partially replacing river sand with textile waste. The two forms of textile waste were cut and ground and cut pieces of 1 cm x 2.5 cm were incorporated to replace 25% sand on volume. The cement block was tested for mechanical properties such as compressive strength, stress-strain characteristics and results were acceptable. Even though concrete with cut and ground textile showed slightly higher compressive strength, it is difficult to use for construction due to its additional cost of production. All the samples showed softening, thus requiring further long-term testing with the improvements to have a better surface finish (Figure 2.5).



Figure 2.5: Surface appearance of fabric incorporated cement block [10]

Spadea et al. [11] investigated engineering applications of recycled nylon fibers obtained from waste fishing nets as tensile reinforcement of cementitious mortars. Fibers were manually cut into three different sizes (13 mm, 25 mm, 38 mm by length and aspect ratio was 39, 77, and 116 respectively) and hand-mixed with dry materials to cast prisms. Fiber incorporation leads to significant improvement of the tensile strength (up to +35%) and fracture properties of cement-based specimens. Reinforcing effect of the fibers in the cement matrix transforms its failure mode to a more ductile one in contrast to the conventional brittle failure mode of cement-based products.

Fantilli et al. [12] experimented with the reinforcing effect of wool fibers in cement-based mortar. Wool fibers of 16 mm length and 19 μm in average diameter were used in their study. Plasma treatment was performed to modify the surface of wool fibers to increase the wettability without affecting the properties of wool filaments. The surface texture of treated and non-treated wool fibers is shown in Figure 2.6. Hemp fibers were used to evaluate the performance of wool fibers as a comparison. Untreated and atmospheric plasma treated fibers were used as reinforcements in casting mortar prism samples to measure the reinforcing effect through a three-point bending test. Reinforcing effect was evaluated based on the results obtained for flexural strength, ductility and fracture toughness. Accordingly, plasma treatment for wool fibers does not significantly affect the mechanical properties of cementitious mortar. Therefore wool fibers, treated and untreated (1% in volume) increase fracture toughness in bending by 300% and the flexural strength by 23% and 18% respectively.

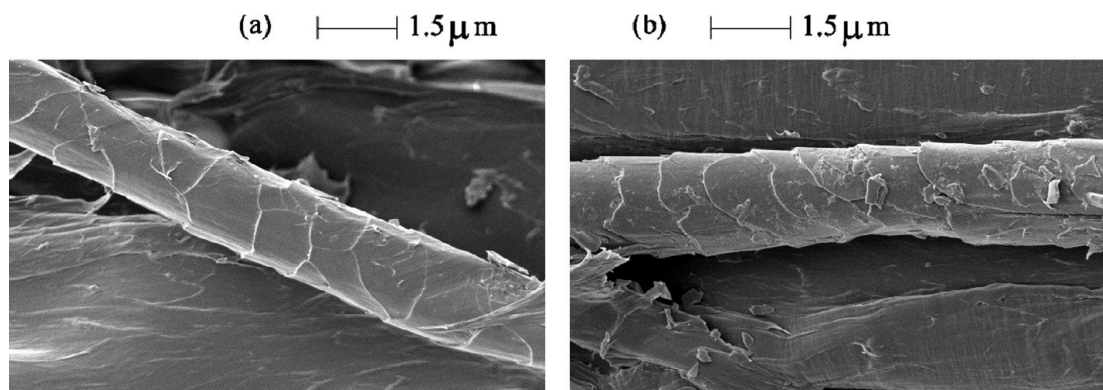


Figure 2.6: The wool filaments used as fiber-reinforcement: (a) non-treated wool; (b) treated wool [12]

Asdrubali et al. [13] reported the state of the art building insulation products made from natural or recycled materials. Thermal and sound insulation materials were developed with the use of recycled textile fibers. The thermal conductivity of recycled cotton fiber products is between 0.039 and 0.044 W/mK. Recycled denim fibers show high sound absorption characteristics. The thermal conductivity of polyester and polyurethane samples were between 0.041 and 0.053 W/mK. The specific heat value of commercialized products made with recycled textile fibers is 1600 J/kgK. Accordingly, it is possible to use textile fibers bonded with synthetic glue for the manufacturing of insulation panels for the construction industry.

CHAPTER 03

3 EXPERIMENTAL INVESTIGATION

3.1 Materials

Polyester spandex fabric offcuts were obtained from one of the leading clothing manufacturers in Sri Lanka. Fabric offcuts were cut into small pieces with the use of a fabric shredding machine and shredded form of fabric pieces (Figure 3.1) were used throughout the experiments.

The size distribution of fabric pieces was analyzed through mechanical sieving with the use of 10mm, 5mm, 4mm and 1.18mm sieves. Considering the flexibility and deformability characteristics of the fabric pieces, its size was analyzed through image analysis with the use of ArcGIS software. In the image analysis, a photograph of randomly selected fabric pieces was taken with the scale of length. Then, the surface area of each fabric piece was calculated according to the actual length scale. Thereafter, the fabric pieces were categorized into different size segments considering the calculated surface area.

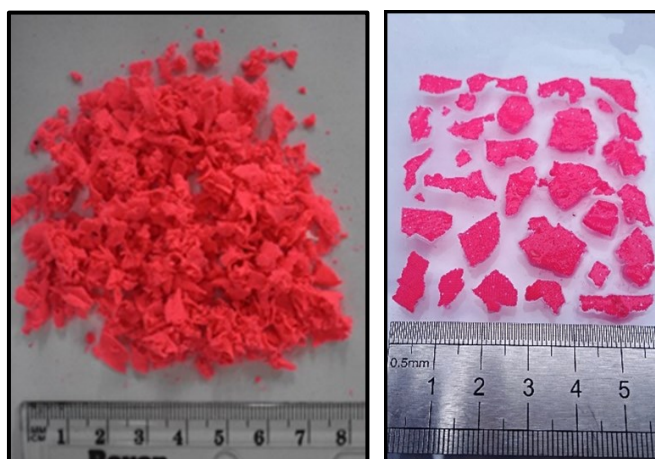


Figure 3.1: Shredded form of fabric pieces

Fiber composition of the polyester-spandex fabric was analyzed in accordance with ISO 1833-1:2006 – “Textiles - Quantitative chemical analysis, Part 1: General principles of testing” [14] for the unique identification of fabric sample used for the experiments.

Weight per unit area of polyester-spandex fabric was measured to determine the thickness of the fabric used in the experiments as per BS EN 12127: [Textiles- Fabrics- Determination of mass per unit area using small samples] [15].

The solid density of polyester-spandex fabric pieces was determined as per SLS 1144 Part 2: [Specification for ready mixed concrete, Part 2: Test methods] [16], which is the method used for determination of solid density of cement. It is important to identify the compatibility of fabric pieces in the cement matrix and to convert the weight-based mix proportions to volume-based mix proportions to get a clear idea of the number of ingredients in the product.

Commercially available Ordinary Portland Cement was used throughout this experiment. The particle density of cement was measured as per SLS 1144 Part 2: [Specification for ready mixed concrete, Part 2: Test methods] [16].

The following measurements were considered for the density calculation of cement and fabric.

m1 - Mass of empty density bottle (g)

m2 - Mass of the density bottle with water (g)

m3 - Mass of the density bottle with kerosene (g)

m4 - Mass of the density bottle with kerosene & cement/ fabric (g)

m5 - Mass of the density bottle with cement/ fabric (g)

Hence, the particle density is calculated with the use of equation 1.

$$\text{Density (kg/m}^3\text{)} = \frac{(m5-m1) \times (m3-m1)}{(m5+m3-m4-m1) \times (m2-m1)} \times 1000 \dots\dots\dots \text{Eq.1}$$

Two separate portions from each sample were used to measure density. If the two density values obtained for the same sample differ by more than 30 kg/m³, fresh measurements were taken for density determination while discarding previous results.

Manufactured sand was used as the fine aggregate for fabric-cement mixtures. The particle size distribution of manufactured sand was analyzed as per BS 812 Part 103.1: [Testing aggregates, Part 103.1 Methods for determination of particle size distribution- sieve tests] [17].

Particle density and water absorption of manufactured sand were analyzed with the use of pycnometer in accordance with BS 812 Part 2: [Sampling and testing of mineral aggregates, sands and fillers, Part 2 - Physical properties] [18].

The following measurements were taken for particle density and water absorption calculation of manufactured sand.

A - Mass of the saturated surface-dry aggregate in the air (g)

B - Apparent mass in the water of the basket containing the sample of saturated aggregate (g)

C - Apparent mass in the water of the empty basket (g)

D - Mass of the oven-dried aggregate in the air (g)

Hence, particle density on an oven-dried basis was calculated with the use of equation 2 and water absorption was calculated in accordance with equation 3.

$$\text{Density (kg/m}^3\text{)} = \frac{D}{A - (B - C)} \dots\dots\dots \text{Eq.2}$$

$$\text{Water absorption (\%)} = \frac{(A - D) \times 100}{D} \dots\dots\dots \text{Eq.3}$$

Poly-carboxylic ether based superplasticizer was used as the water-reducing admixture in fabric-cement composites. Cellulose-based viscosity modifier was used to improve the homogeneity of fabric-cement composites.

Water that does not taste saline or brackish in which P^H is in the range of 6.0 to 8.0 was used as the mixing water.

3.2 Casting of tile samples

Tile samples (size 100 mm x 100 mm x 10 mm) were cast to observe the dispersion of fabric pieces in the cement matrix. Incorporated fabric content was kept as 16%, 23% and 28% by volume. Water: cement ratio was increased from 0.53 to 0.78 with the increase of fabric percentage in order to obtain sufficient workability to compact the mix.

As the initial step of the casting process, shredded form of fabric pieces were mixed in dry state with cement according to the mix proportions tabulated in Table 3.1 until the

surfaces of fabric pieces covered with cement powder. Then water was added to the mixture until required consistency was achieved and the homogenized mixture was placed into moulds with manual compaction to cast tile samples. The condition of the mixture during the initial steps in the casting process is shown in Figure 3.2. Cast specimens were de-moulded after 24 hours from casting at room temperature.

Table 3.1: Mix proportions used for casting fabric incorporated tile specimens

Sample ID	W/C	Fabric % by volume
FV16/0.53	0.53	16
FV16/0.72	0.72	16
FV23/0.72	0.72	23
FV23/0.78	0.78	23
FV28/0.72	0.72	28
FV28/0.78	0.78	28



(a) Dry form of a fabric-cement mixture



(b) Fresh homogenized mixture for tile casting



(c) Cast tile samples in two gang square mould

Figure 3.2: Steps used for casting of tile samples

3.3 Casting and testing of cement paste prisms

3.3.1 Casting procedure

Cement paste prism samples (size: 40 mm x 40 mm x 160 mm) were cast for flexural strength and compressive strength tests. Shredded form of fabric, cement, water and admixtures were used for casting of cement paste specimens.

Two types of admixtures were used as given below.

1. Powder form Cellulose-based viscosity modifier – (Mecellose)
2. Liquid form Poly-carboxylic ether based superplasticizer – (Hypercrete)

Initially, required material quantities were weighed considering the mix proportion. Then the liquid form of admixture was properly mixed with the measured quantity of water and in the meantime powder form of admixture was manually mixed with approximately half weight of the cement content. Thereafter, admixture and water mixture were added to admixture and cement mixture and properly mixed to form a viscous cement slurry. Then shredded fabric pieces were added to the cement slurry and mechanical mixing was performed until fabric pieces were properly covered with cement paste. Then the remaining cement portion was added into the mixture and the mixing was continued until a homogeneous mixture was obtained. A mortar mixer complies with the requirements specified in SLS ISO 679: [Test methods for cements – Determination of strength] [19] was used for mechanical mixing.

Three gang prism moulds were used for casting of cement paste specimens and compaction was achieved by using jolting apparatus. The homogenized mixture was placed in the prism moulds in two layers and each layer was compacted by applying 60 jolts within a time period of 60 seconds.

Properly filled and compacted moulds were removed from the jolting apparatus and the top surface was leveled with the use of a trowel. Cast specimens were kept in the mould for 24 hours without any disturbance at room temperature. The top surface of the mould was covered by a glass plate to minimize water evaporation during the initial stage of curing. After completion of 24-hour initial curing period, cast specimens were de-moulded and immersed in water for curing until the flexural or compression

strength test was performed. Different stages in the casting procedure are shown in Figure 3.3.



(a) Viscous cement slurry
(Cement + admixture + water)



(b) Fabric pieces covered with
cement paste



(c) Homogenized mixture ready for casting of prism specimens



(d) Prism moulds after filling
and compacting first layer



(e) Cast prism specimens ready
for curing



(f) Demoulded prism specimen

Figure 3.3: Casting procedure of cement paste prism samples

Mix proportions were altered by changing admixture type, fabric content and size of fabric pieces. Each factor was changed once while keeping the other factors unchanged. Mix proportions used for casting of fabric embedded cement paste prism samples were tabulated in Tables 3.2, 3.3 and 3.4.

Table 3.2: Mix proportions used for selection of suitable admixtures

Mix ID	W/C	Fabric % by volume	Cement % by volume	C type admixture % by weight of cement	H type admixture % by weight of cement
FV23/0.5	0.5	23	77	-	-
FV23/0.5/C	0.5	23	77	0.3	-
FV23/0.5/H	0.5	23	77	-	0.6
FV23/0.5/C,H	0.5	23	77	0.3	0.6

Table 3.3: Mix proportions used for selection of suitable fabric incorporation

Mix ID	W/C	Fabric % by volume	Cement % by volume	C type admixture % by weight of cement	H type admixture % by weight of cement
FV05/0.5/C,H	0.5	05	95	0.3	0.6
FV10/0.5/C,H	0.5	10	90	0.3	0.6
FV15/0.5/C,H	0.5	15	85	0.3	0.6
FV20/0.5/C,H	0.5	20	80	0.3	0.6
FV25/0.5/C,H	0.5	25	75	0.3	0.6
FV26/0.5/C,H	0.5	26	74	0.3	0.6
FV28/0.5/C,H	0.5	28	72	0.3	0.6
FV30/0.5/C,H	0.5	30	70	0.3	0.6
FV35/0.5/C,H	0.5	35	65	0.3	0.6

Table 3.4: Mix proportions used for selection of suitable sizes of fabric pieces

Mix ID	W/C	Fabric % by volume	Size segment of fabric pieces (mm)	Cement % by volume	C type admixture % by weight of cement	H type admixture % by weight of cement
F0-2/0.5/C,H	0.5	26	0-2.0	74	0.3	0.6
F2-3.5/0.5/C,H	0.5	26	2.0-3.5	74	0.3	0.6
F3.5-4/0.5/C,H	0.5	26	3.5-4.0	74	0.3	0.6
F4-5/0.5/C,H	0.5	26	4.0-5.0	74	0.3	0.6
F5-6.3/0.5/C,H	0.5	26	5.0-6.3	74	0.3	0.6
F6.3-8/0.5/C,H	0.5	26	6.3-8.0	74	0.3	0.6
F8-10/0.5/C,H	0.5	26	8.0-10	74	0.3	0.6
F10-12.5/0.5/C,H	0.5	26	10-12.5	74	0.3	0.6
F12.5-14/0.5/C,H	0.5	26	12.5-14	74	0.3	0.6

3.3.2 Flexural strength

Flexural strength test was performed for the specimens at saturated surface dry condition, under three-point loading according to the method described in SLS ISO 679: [Test methods for cement - Determination of strength] [19].

The following equation was used in the calculation of flexural strength [19].

$$R_f(\text{MPa}) = \frac{1.5 \times F_f \times l}{b^3} \dots\dots\dots \text{Eq.4}$$

b – Side length of the square section of the prism (mm)

F_f – Load applied to the middle of the prism at fracture (N)

l – Distance between the supports (mm)

3.3.3 Compressive strength

A compressive strength test was carried out on the halves of the prism broken under the flexural strength test, as per the method described in SLS ISO 679: [Test methods for cement - Determination of strength] [19]. The moisture content of the test specimens was maintained as a saturated surface dry condition.

Compressive strength R_c was calculated considering the following equation.

$$R_c(\text{MPa}) = \frac{F_c}{1600} \dots\dots\dots \text{Eq.5}$$

F_c – Maximum load at fracture (N)

1600 – Area of the platen (40 mm x 40 mm)

3.4 Casting and testing of paving blocks

3.4.1 Casting procedure

Paving block samples (size: 200 mm x 100 mm x 60 mm) were cast with the use of a shredded form of fabric, cement, manufactured sand (quarry dust), water and admixtures. Plastic moulds, mechanical mixing, manual compaction and mechanical vibration were used for casting of paving blocks.

Initially, material quantities were weighed according to the required mix proportion. The material mixing procedure is the same as the procedure described in section 3.3.1.

The liquid form of admixture (superplasticizer) was properly mixed with water (water content was measured by considering w/c ratio as 0.6). Manufactured sand was added to the mixture at the time of adding the remaining cement portion and ingredients were properly mixed to get a homogeneous mix. The workability of the fresh mixture was measured with the use of cone penetrometer and water content was adjusted to achieve the required workability. Penetration depth was maintained in the range of 7 mm -11 mm by means of the failing weight of 150g. Depth of penetration was measured after completion of 30 seconds time period since the weight has fallen from the top surface of the mixture as indicated in Figure 3.4.

The homogenized mixture was placed into plastic moulds in two layers and manual compaction was done with the use of the tamping rod. Thereafter, further compaction was achieved through vibration by using a vibrating table where moulds were clamped to the vibrating table.

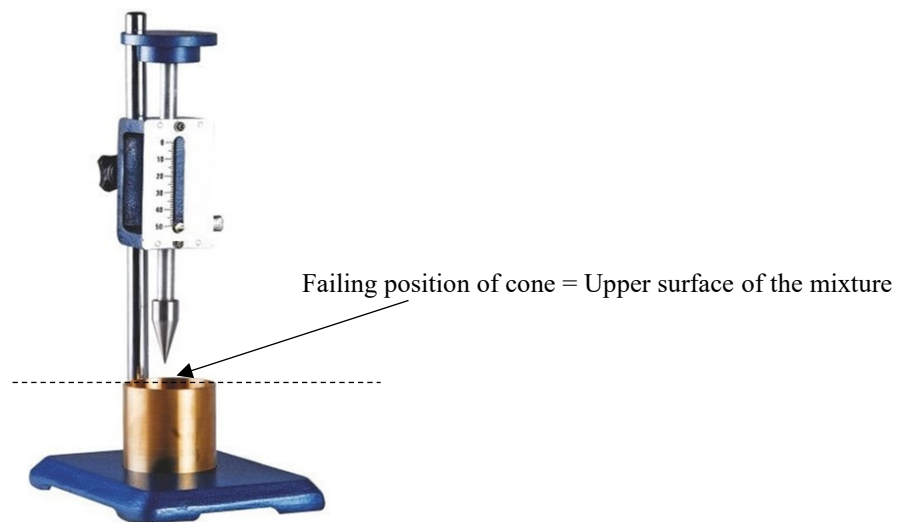


Figure 3.4: Cone penetrometer

Cast paving blocks were kept in the moulds for 12 hours without any disturbances in the laboratory at room temperature. Cast paving blocks were de-moulded after completion of minimum 12 hours' time period and those blocks were immersed in water after completion of 24 hours from casting time, for further curing until performing the required test. Important steps in the casting procedure of fabric embedded paving blocks are shown in Figure 3.5.

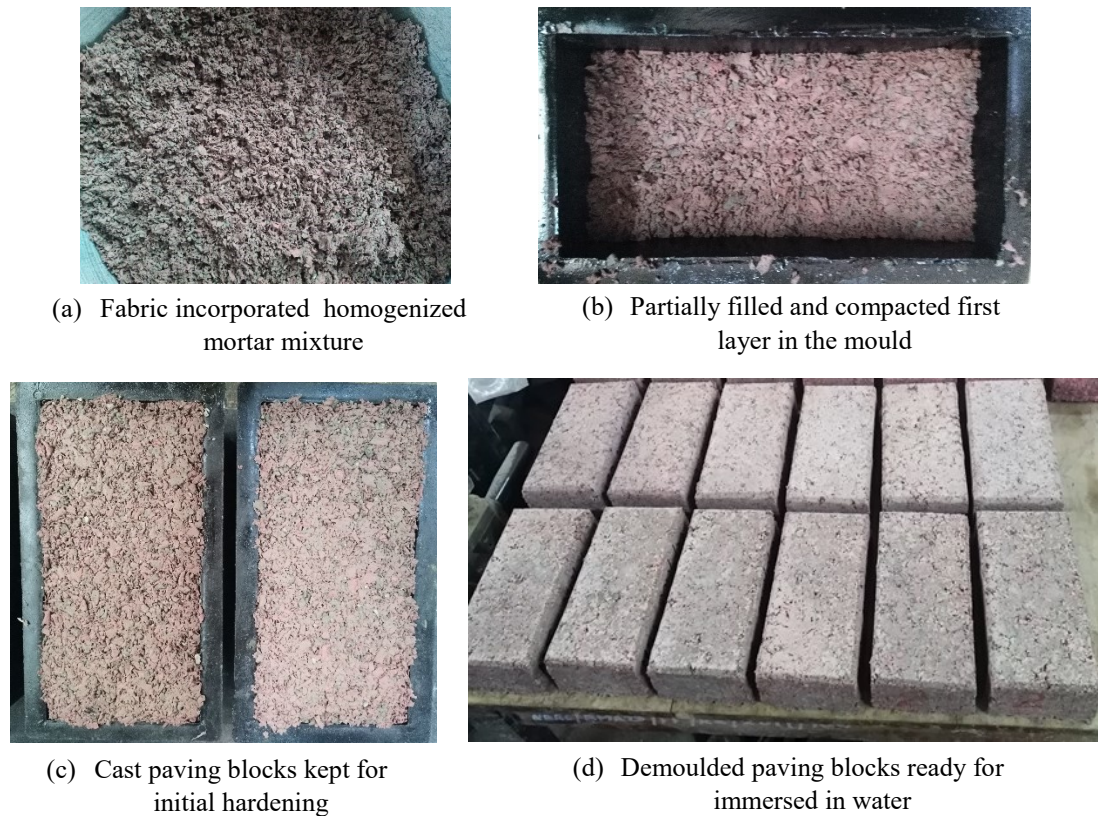


Figure 3.5: Casting procedure of paving blocks

3.4.2 Compressive strength

Length and width measurements of each specimen were recorded at the initial stage for the calculation of the plan area required for strength calculation. The test was performed for the specimens at the saturated surface dry condition.

The compression load was applied to the specimen at a constant rate of 15 N/mm min. The load was applied to the specimen through steel plates placed on the upper and lower surfaces of the specimen. Steel plates used were 5 mm thick and larger than specimen by a margin of 20 mm at all edges. The failure load of each specimen was recorded for the calculation of compressive strength. Compressive strength was calculated by dividing the failure load by plan area and multiplying the resulting value by 1.06 to account for the presence of chamfered edges on 60 mm thick block in accordance with SLS 1425, Part 2: [Specification for concrete paving blocks, Part 2 - Test methods] [20].

Compression test of fabric embedded paving block is shown in Figure 3.6.

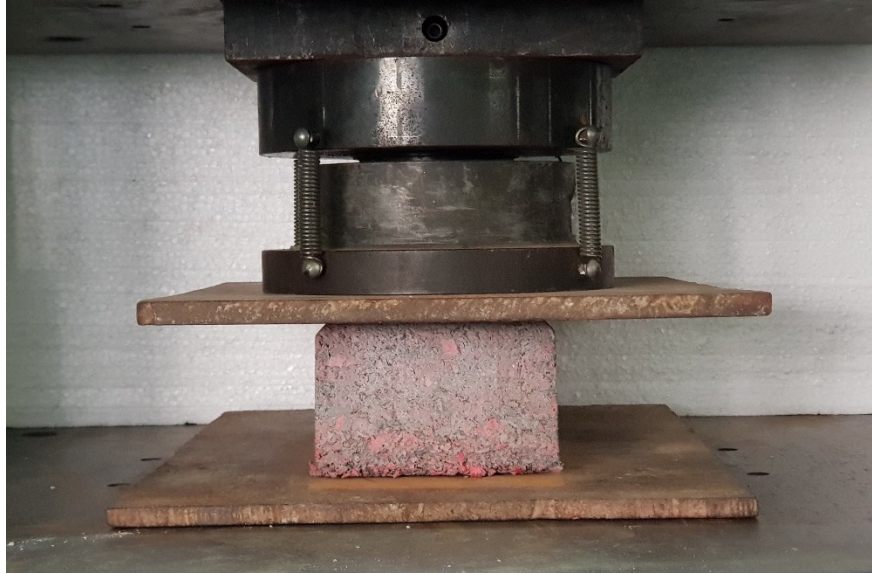


Figure 3.6: Compression test of paving block

3.4.3 Tensile splitting strength

The test was performed for the paving blocks at the saturated surface dry condition and the splitting section was selected as a $200\text{ mm} \times 60\text{ mm}$ area at the center of the specimen as indicated in Figure 12.

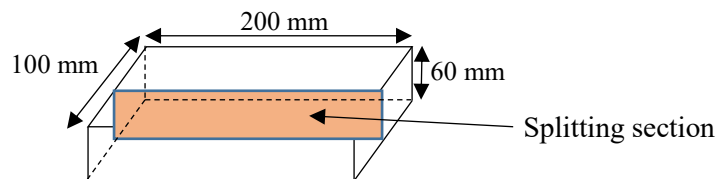


Figure 3.7: Splitting section of the test specimen

Compression load was applied to the splitting section from upper and lower surfaces of the specimen at a rate of 0.05 MPa/s according to the method described in BSEN 1338: [Concrete paving blocks - Requirements and test methods] [21].

Tensile splitting strength test of fabric embedded paving block was shown in Figure 3.8.

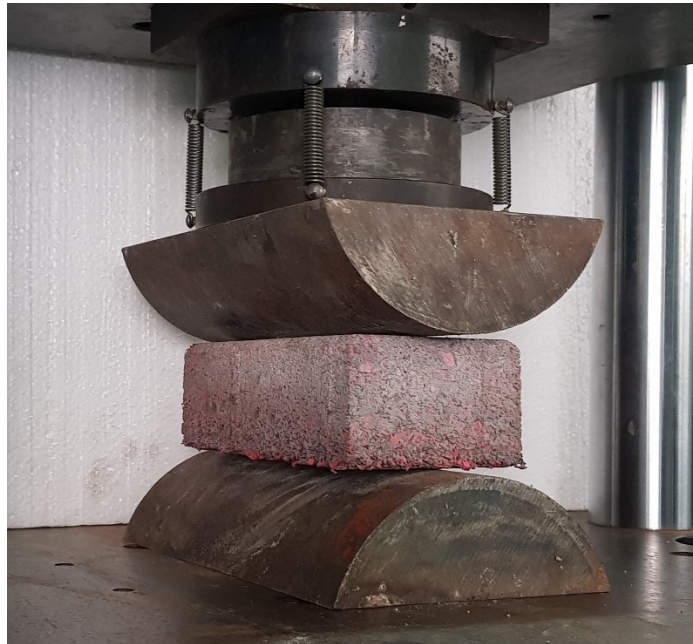


Figure 3.8: Tensile splitting test of paving block

Failure load was recorded and tensile splitting strength was calculated as follows.

The equation 6 used for calculating the area of the failure plane of the block;

$$S = l \times t \dots\dots\dots \text{Eq.6}$$

S – Area of the failure (mm²)

l – Mean of two measurements of the failure length, one at top and one at the bottom of the block (mm)

t – Thickness of the block at the failure plane, mean of the three measurements one in the middle and one at either end (mm)

Calculation of tensile splitting strength of paving bock;

$$T = 0.637 \times k \times \frac{P}{S} \dots\dots\dots \text{Eq.7}$$

T – Tensile splitting strength (MPa)

P – Failure load (N)

k – Correction factor for the block thickness (when t = 60 mm, k = 0.87)

3.4.4 Abrasion resistance

Abrasion resistance was measured using a wide wheel abrasion tester (see Figure 3.9) according to the method specified in BSEN 1338: [Concrete paving blocks - Requirements and test methods] [21]. The test was performed using paving blocks in dry condition with the use of standard sand complies with ISO 8486-1: [Bonded abrasives – Determination and designation of grain size distribution]. Test was performed for the upper face of the specimens at dry conditions belongs to selected mix proportions. Abrasion resistance was measured by measuring the dimensions of the abraded groove.



Figure 3.9: Wide wheel abrasion tester

3.4.5 Skid resistance

Skid resistance test was performed to determine the Unpolished Slip Resistance Value (USRV) of the paving blocks with the use of pendulum friction tester (Figure 3.10). The test was performed for specimens at a wet condition in accordance with the method specified in BSEN 1338: [Concrete paving blocks - Requirements and test methods] [21].



Figure 3.10: Pendulum friction test equipment

Pendulum value was recorded for each specimen and the mean pendulum value obtained for 5 specimens was taken as the USRV.

3.4.6 Permeability

Permeability test was performed to determine the relative permeability of fabric embedded paving blocks. Permeability was measured in terms of its infiltrated water volume at constant time intervals under constant pressure head [22].

Cylindrical shape samples (diameter = 75 mm and height = 60 mm as shown in Figure 3.11) cut from cast paving blocks with the use of core cutting machine were used as test specimens. Saturated test specimens were used for the test. In this test, water was allowed to flow through a column of cylindrical test piece under constant pressure conditions and the amount of water permeate through the test specimen was collected and measured at constant time intervals.

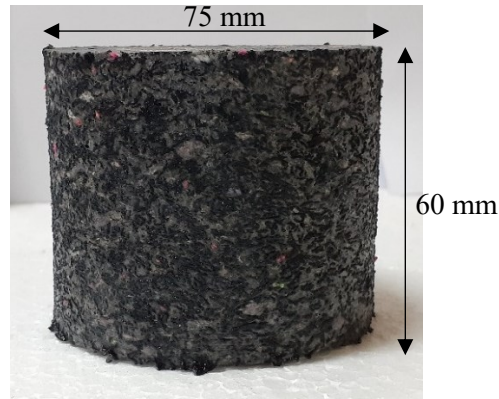


Figure 3.11: Cylindrical shape test specimen

The test apparatus is shown in Figure 3.12, which consists of an adjustable constant head (height of water column can be kept as 500 mm, 1000 mm and 1500 mm) and outlets for maintaining a constant head during the test. The cylindrical surface of the test piece was sealed using a rubber sheet to prevent water leakage through the edges of the test piece.

The saturated test specimen was placed in the cylindrical cell and tightened to seal its cylindrical surface to prevent water flowing through the surface. Then the constant head tube was connected to the cylindrical cell and tightened to prevent water leakages. Thereafter, water flow was connected to the water inlet tube and the appropriate valve was opened to control the required pressure head. Percolated water through the specimen was collected using a flask at every 30 minutes intervals for a period of 3 hours.

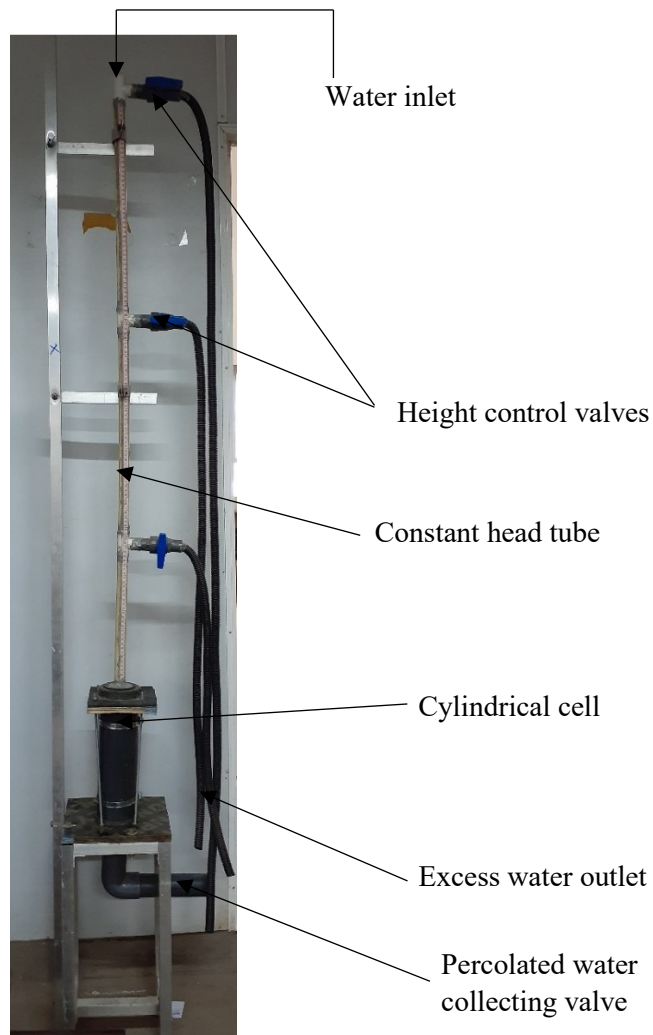


Figure 3.12: Constant head permeameter

3.4.7 Shock absorption

Shock absorption capability of fabric embedded paving blocks was measured using Artificial Athlete Apparatus (AAA) in accordance with the method scribed in BSEN 14808: [Surfaces for sports areas – Determination of shock absorption] [23]. Shock absorption was determined by applying an impact force through a spring to the test specimen. The load was measured using a load cell placed under the spring and a dynamic data logger was used to record the generated maximum impact forces. The main components of the Artificial Athlete Apparatus is shown in Figure 3.13.

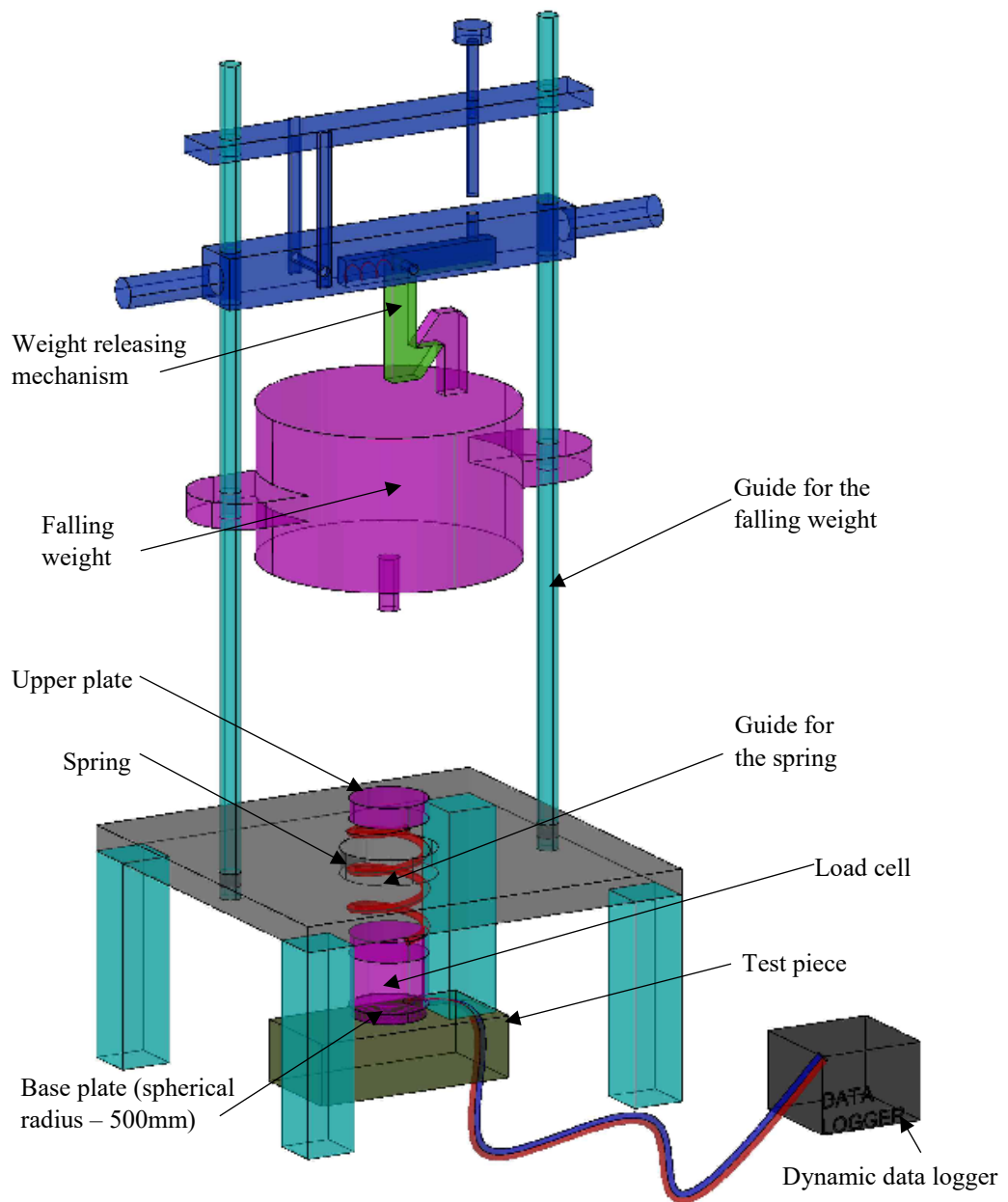


Figure 3.13: Designed shock absorption test apparatus

Shock absorption was measured based on its force reduction capability. Force reduction was measured using AAA which consists of a falling mass of 20 kg. The impact force was transferred to the measuring surface through a spring with stiffness of 770 N/mm. Stiffness of the spring was measured by analyzing its load-deformation values as shown in Figure 3.14.

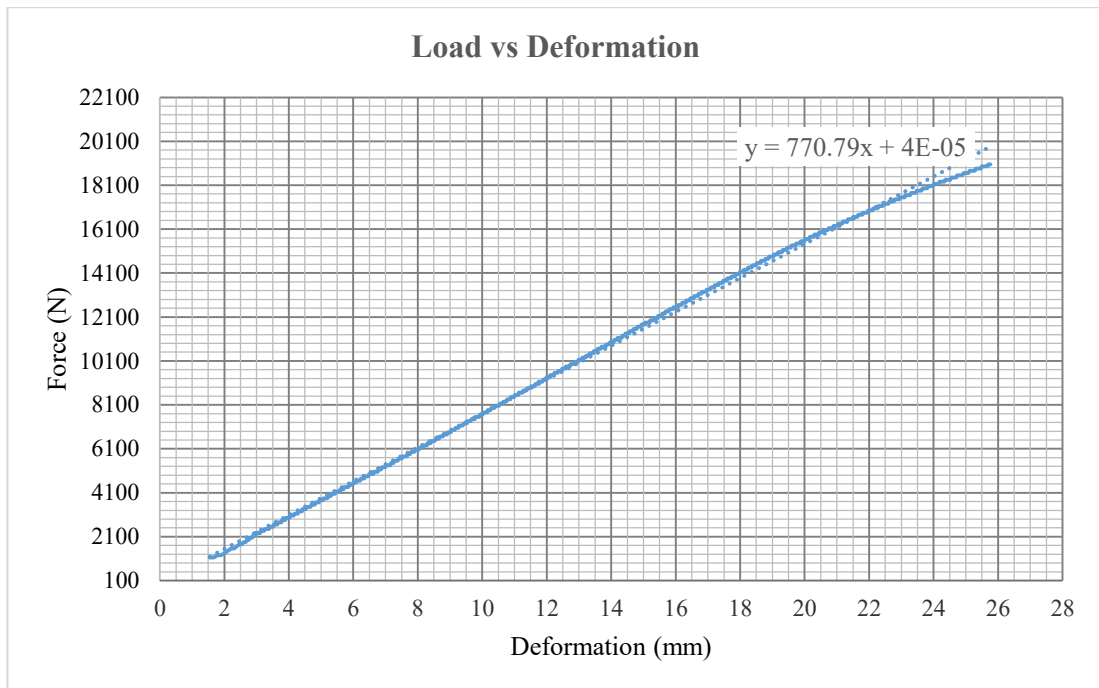


Figure 3.14: Load deformation variation of spring

The load cell was placed directly beneath the spring and load cell was connected to the dynamic data logger to record the forces generated during an impact. Impact force was applied to the test piece as a point load through a 500 mm radius spherical surface of a metal plate.

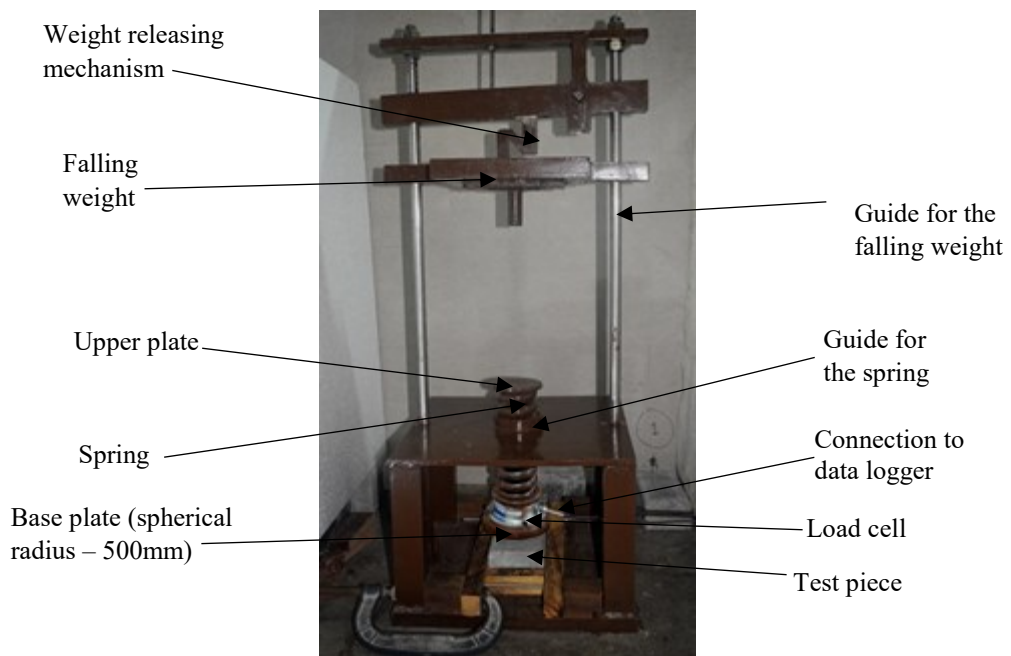


Figure 3.15: Fabricated Artificial Athlete Apparatus

Fabricated Artificial Athlete Apparatus, which is ready for shock absorption measurement is shown in Figure 3.15.

The apparatus was designed to automatically release the falling weight (20 kg) at 250 mm height from the top surface of the upper plate (Figure 3.15). Accordingly energy of falling mass at impact point equals to its kinetic energy. The potential energy of the weight is converted to kinetic energy during its movement. Therefore impact velocity can be calculated based on the potential energy difference of the falling weight as follows.

m – mass of the falling weight

g – acceleration due to gravity

v – impact velocity

$$\begin{aligned}m \times g \times h &= \frac{1}{2} \times m \times v^2 \\g \times h &= \frac{1}{2} \times v^2 \\9.81\text{ms}^{-2} \times 0.25\text{m} &= 0.5 \times v^2 \\v &= 2.215\text{ms}^{-1}\end{aligned}$$

Velocity at the time of impact is 2.215 m/s.

The concrete surface was considered as the rigid surface to evaluate the shock absorption capability of fabric embedded paving blocks [23]. AAA was set on the concrete surface and impact force was measured. Measured impact force corresponding to the concrete surface was used as the baseline to calculate the force reduction of the fabric embedded paving blocks.

The theoretical maximum force generated on the rigid surface can be calculated based on the following assumptions [24].

- Spring mass is negligible (actual mass of the spring does not contribute to deflection of the spring).
- Spring is an ideal one (its deflection is completely linear during its response)
- Materials are ideal (infinite hardness, no linear or plastic deformation and no internal material damping).

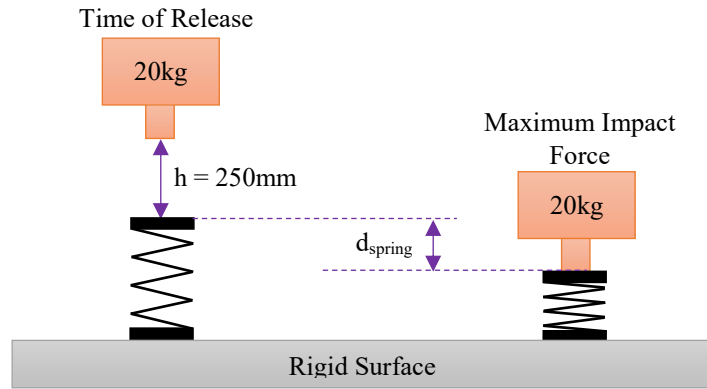


Figure 3.16: Moving system of artificial athlete apparatus

The total vertical distance traveled by the falling weight (H) is calculated as follows.

$$H = h + d_{\text{spring}}$$

h - free fall distance specified (250 mm) in BSEN 14808 [23]

d_{spring} – compression of spring due to impact force

Potential energy reduction of falling weight is calculated as follows.

$$\begin{aligned} E_{\text{mass}} &= m \times g \times H \\ &= 20 \times 9.81 \times (0.25 + d_{\text{spring}}) \\ &= 196.2 \times (0.25 + d_{\text{spring}}) \end{aligned}$$

Reduced potential energy (E_{mass}) is equal to the energy in the spring (E_{spring}) after impact. Accordingly, deflection of the spring can be calculated as follows.

k – spring constant

$$\begin{aligned} E_{\text{mass}} &= E_{\text{spring}} \\ 196.2 \times (0.25 + d_{\text{spring}}) &= \frac{1}{2} \times k \times (d_{\text{spring}})^2 \\ 196.2 \times (0.25 + d_{\text{spring}}) &= 0.5 \times (770 \times 1000) \times (d_{\text{spring}})^2 \\ 1000(d_{\text{spring}})^2 - 0.5096 \times (d_{\text{spring}}) - 0.1274 &= 0 \end{aligned}$$

Above quadratic equation had two real solutions;

$$d_{\text{spring}} = 0.011545 \text{ m}$$

$$d_{\text{spring}} = -0.011035 \text{ m}$$

Negative solution does not fit for this impact model because spring cannot expand due to compression type impact force. Therefore, positive solution (0.011545 m) was considered as deflection of the spring due to impact force.

Accordingly, the theoretical maximum force generated on the test surface is calculated with the use of spring constant and its deflection.

$$\begin{aligned} F &= k \times d_{\text{spring}} \\ &= (770 \times 1000) \times 0.011545 \\ &= 8890 \text{ N} \end{aligned}$$

This theoretical maximum force was calculated based on the assumptions stated earlier. Therefore actual force values obtained during the test can be higher than the above-calculated value due to the deviation of assumed conditions from real conditions. However, this estimation is useful to get a clear idea of the capacity of a suitable load cell. Accordingly, it was decided to use a 1-ton compression type load cell to measure impact force in the shock absorption test. Practical deviations on maximum impact load around 10000 N are acceptable based on 150% safe overload limit and 300% ultimate overload limit of the load cell. The selected load cell model was H2F-C3-1t-3T6 (Zemic brand). The use of a dynamic type data logger to record generated impact forces is very important due to its high range of sampling frequency. Accordingly, EDX-100A type Kyowa dynamic data logger that has the capability to record generated data at 1 second - 0.000001 second time intervals, was used in this study.

The test specimens were paved on a leveled surface and properly compacted base with the use of ABC and fine aggregate (crushed rock sand). The test was performed using four numbers of specimens belong to selected mix proportions of fabric embedded paving blocks at site condition and the maximum impact force observed for each specimen was considered for calculations.

Initially, impact force obtained for concrete surface was considered as a baseline to calculate the force reduction of fabric embedded paving blocks. Then, the apparatus was set up on the fabric embedded paving blocks paved surface and the test was

performed to record the maximum impact force generated on the test surface. Force reduction was calculated using the following equation.

$$R = \left(1 - \frac{F_t}{F_r}\right) \times 100$$

R – Force reduction %

F_t – Observed maximum force for test piece (N)

F_r – Observed maximum force for concrete (N)

3.4.8 Durability

The durability of the product mainly depends on its material composition and environmental exposure conditions. The composition of developed paving blocks varies at the point of incorporation of polyester-spandex fabric pieces when compared with conventional concrete paving blocks. Fabric pieces act as reinforcing fibers in the fabric embedded paving blocks. Therefore, durability evaluation was mainly focused on the deterioration of fabric pieces in the cement matrix.

The durability of conventional cement-based paving blocks was evaluated through the water absorption test, but this method is not suitable for permeable paving blocks due to the high amount of porosity and water percolation of the block. Therefore, durability of fabric embedded paving blocks was considered under moist and temperature conditions.

3.4.8.1 Durability under moist and temperature conditions

Effect of moisture and temperature on the deterioration of textile fibers in the cement matrix was evaluated through the performance of 50 numbers of soak-dry cycles according to the method described in ISO 8336: [Fiber cement flat sheets – Product specification and test methods] [25]. Four numbers of paving block specimens belonging to each mix proportion were subjected to soak-dry cycles under the following conditions.

Specimens were first immersed in water at ambient temperature for 18 hours. After that, those samples were removed from water and kept in the oven at 60⁰C for 6 hours.

These soak-dry cycles were repeated 50 times as the accelerated durability test. Four numbers of conventional concrete paving blocks were also subjected to the same soak dry cycles at the same conditions together with fabric embedded paving blocks belonged to selected three mix proportions.

Reinforcing effect of textile fibers of these specimens can be directly evaluated by performing tensile splitting strength test according to the method described in BSEN 1338: [Concrete paving blocks – requirements and test methods] [21].

Accordingly, deterioration of fabric embedded paving blocks were evaluated by splitting tensile strength testing of samples subjected to accelerated durability conditions. Soak-dry performance criteria were calculated based on tensile splitting strength results of specimens in the condition of before soak-dry performance and after the soak-dry performance as mentioned in ISO 8336 [25]. The methodology used for the calculation of soak-dry performance is described as follows.

The tensile splitting strength ratio was calculated for each pair of specimens according to the following equation.

$$\text{Tensile splitting strength ratio} = \frac{\text{Tensile splitting strength of the } i^{\text{th}} \text{ specimen after soak-dry cycles}}{\text{Tensile splitting strength of the } i^{\text{th}} \text{ specimen before soak-dry cycles}}$$

Average and standard deviation were calculated for each mix ID using the calculated individual tensile splitting strength ratio values. Then soak-dry performance criteria were calculated at lower estimation, considering the 95% confidence level with the use of the following equation.

$$\text{Soak-dry performance criteria} = \text{Average tensile splitting strength ratio} - 0.58 \times \text{Standard deviation}$$

CHAPTER 04

4 RESULTS AND DISCUSSION

4.1 The size distribution of fabric pieces

Initially, size distribution of the shredded form of polyester-spandex fabric pieces was determined through sieve analysis using sieve sizes of 10 mm, 5 mm, 4.75 mm, 4 mm, 2.36 mm, 1.18 mm, 0.6 mm, 0.3 mm and 0.15 mm sieves. Fabric pieces were added to the sieve little by little, considering the difficulties in sieving fabric due to its lightweight nature. Sieve analysis was performed on six randomly selected samples of shredded polyester spandex pieces to confirm the uniformity of the material and considerable deviations were not observed among these samples. Sieve analysis test results obtained for a representative sample is tabulated in Table 4.1.

The initial mass of dry sample = 50 g

Table 4.1: Sieve analysis test results of fabric pieces

Test Sieve (mm)	Mass Retained (g)	Cumulative Mass Retained (g)	Cumulative Percentage Retained	Observed Passing Percentage
10	0	0	0	100
5.0	11.88	11.88	24	76
4.75	15.10	26.98	54	46
4.00	7.98	34.96	70	30
2.36	10.15	45.11	90	10
1.18	3.13	48.24	96	4
0.600	0.66	48.90	98	2
0.300	0.39	49.29	99	1
0.150	0.02	49.31	99	1
Pan	0.15	49.46	99	-

According to the results obtained, a majority of fabric pieces passed through 5 mm sieve and retained on 1.18 mm sieve. Hence, approximately 72% of fabric pieces were lying in the range of 1.18 mm to 5 mm size. The size of all fabric pieces is less than 10 mm.

Graphical representation of the size distribution of fabric pieces is shown in Figure 4.1.

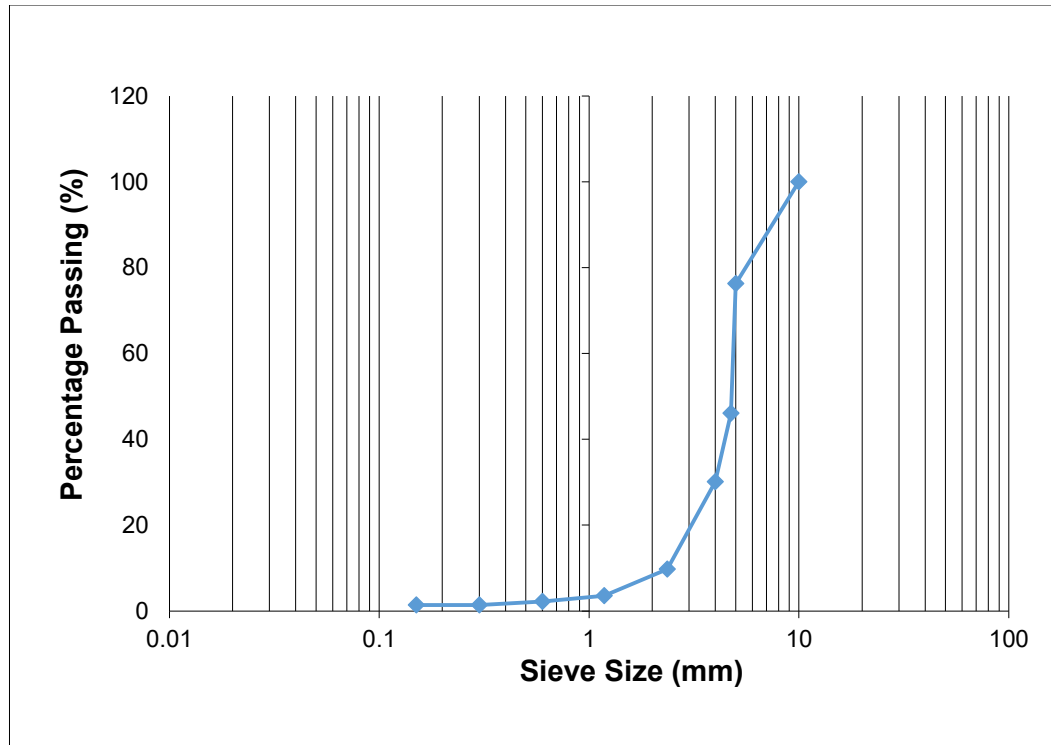


Figure 4.1: Size distribution of shredded fabric pieces

Flexibility and deformability characteristics of fabric pieces affect the accuracy of sieve analysis results on size distribution. Therefore, the size of fabric pieces was analyzed through image analysis with the use of Figure 4.2 by calculating surface area considering the actual dimensions based on the scale represented by rulers in the image.

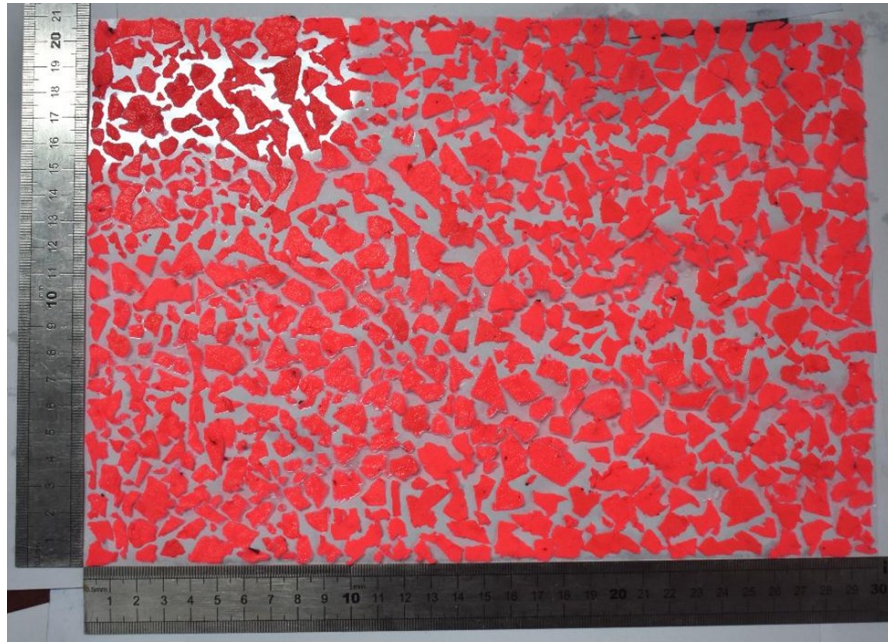


Figure 4.2: Image used for surface area analysis of fabric pieces

The surface area was calculated and fabric pieces were categorized into different size segments as indicated in Figure 4.3. The number of fabric pieces used for this analysis is 577 which was randomly selected to represent the whole sample.

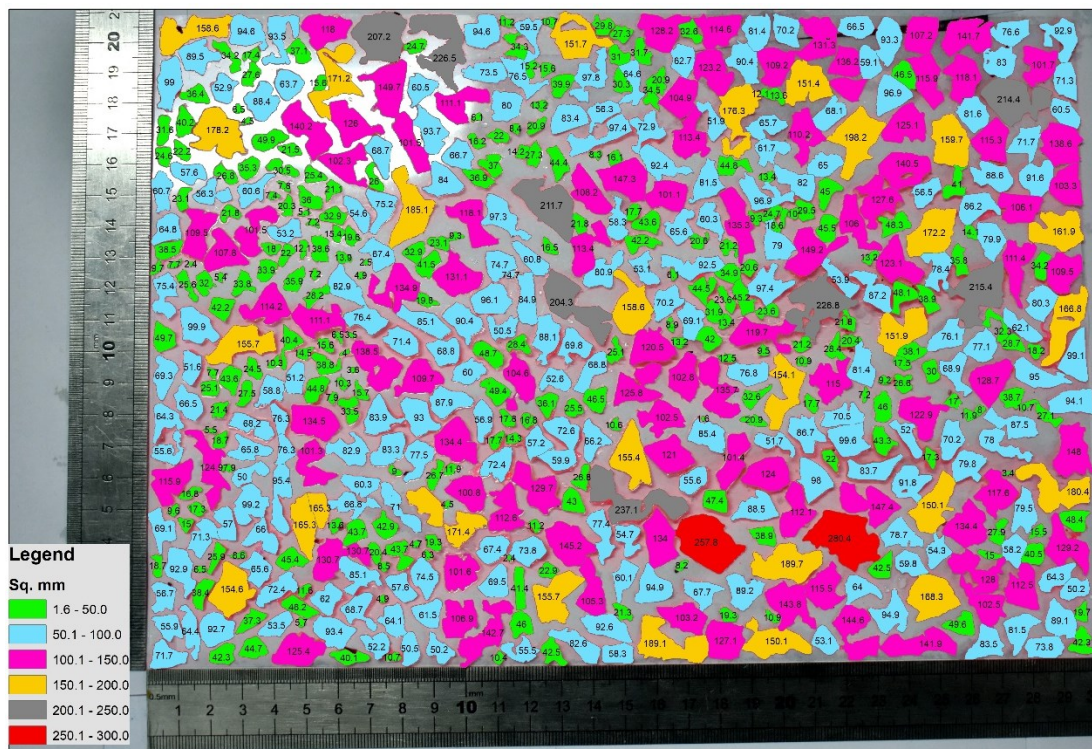


Figure 4.3: Area of analyzed fabric pieces belonged to different size segments

Table 4.2: Results of surface area analysis

Range of area in mm ²	Num. of fabric pieces	% of fabric pieces
0-50	247	42.8
51-100	199	34.5
101-150	93	16.1
151-200	28	4.9
201-250	8	1.4
251-300	2	0.3

Surface area analysis results are summarized in Table 4.2 and these results illustrate that approximately 77.3% of fabric pieces were below 100 mm² size and 98.3% of fabric pieces were less than 200 mm² in size.

4.2 Particle size distribution of sand

Manufactured sand which is a byproduct of a coarse aggregate production was used as the fine aggregate throughout this study. The particle size distribution of manufactured sand was obtained by performing mechanical sieving and the results are tabulated in Table 4.3 and graphically represented in Figure 4.4.

Table 4.3: Sieve analysis test results of manufactured sand

Test Sieve (mm)	10.0	5.0	2.36	1.18	0.600	0.300	0.150	0.075
Passing %	100	99	77	54	41	28	17	11
Specified Requirements for medium graded fine aggregate according to BS 882 : 1992	100	89-100	65-100	45-100	25-80	5-48		0-16

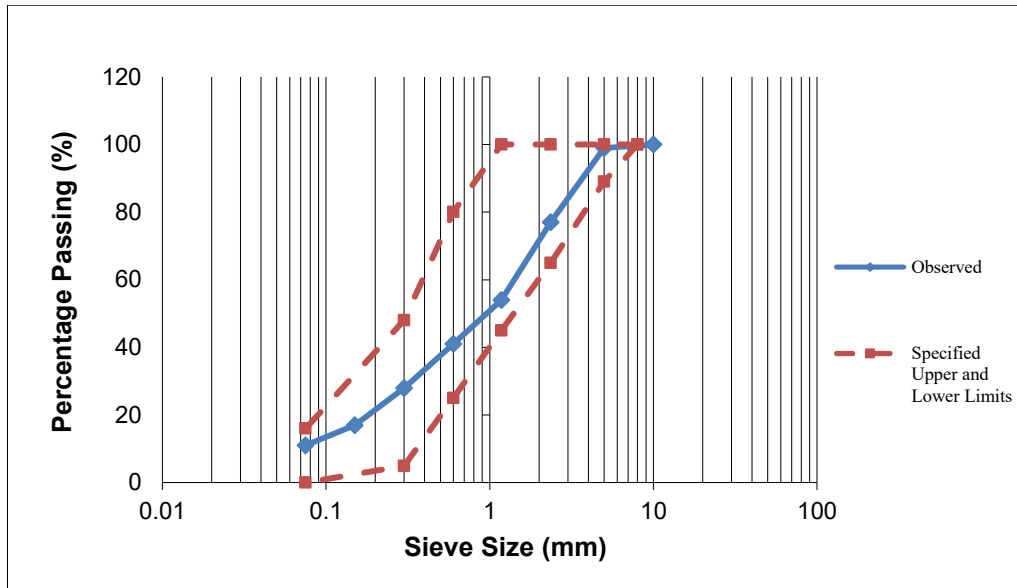


Figure 4.4: Particle size distribution of manufactured sand

Sieve analysis test results and the above figure illustrate that particle size distribution of manufactured sand complies with the requirements specified for medium graded fine aggregate as per BS 882: [Specification for aggregates from natural sources for concrete] [26].

4.3 Fiber composition of polyester spandex fabric

Polyester spandex is a woven fabric with the use of polyester fibers and spandex fibers. Fiber composition is decided after considering the required fabric properties. Accordingly, spandex content of commercially available polyester spandex fabrics varies from 5-40% and the remaining portion is polyester fibers. Therefore, fiber composition was analyzed for the unique identification of fabric samples used in this study as described in section 3.1. Consequently, the fabric sample used for this study was found to contain 9.2% of spandex (elastane) fibers and 90.8% of polyester fibers.

4.4 Weight per unit area of polyester spandex fabric

In this study, fabric samples were used in woven form and not in the fiber form. Therefore, to get an idea about the thickness of the fabric, its grams per square meter (GSM) value was measured using a conditioned sample that is in the relaxed state based on the method described in section 3.1. Accordingly, the GSM of polyester spandex used throughout this study was 141 g/mm².

4.5 Particle density

The particle density of the shredded form of polyester-spandex fabric pieces and ordinary portland cement was measured with the use of a specific gravity bottle as described in section 3.1. The density of shredded fabric was found to be 1386 kg/m^3 and that of cement was 3276 kg/m^3 . It means that, fabric pieces are approximately 57% lighter than the cement. The lightweight attribute of fabric directly affects the homogeneous distribution of fabric pieces in the cement matrix, which leads to the movement of fabric pieces to the upper surface of the product. It was decided to use a viscosity modifying admixture to prevent that movement in order to achieve homogeneous mixture of fabric cement composite.

The particle density of manufactured sand was measured using the pycnometer and it was found to be 2700 kg/m^3 .

Expression of the mix proportions on a volume basis is the most suitable way to get a clear idea of the ingredients in the product. During the experimental investigation mix proportioning was done on weight basis. Later, density measurements were used to convert weight-based mix proportions to volume-based mixtures.

4.6 Dispersion of fabric pieces in the cement matrix

The dispersion of fabric pieces in the cement matrix was visually observed on cast tile samples. Water demand for the mixture was increased with the increment of fabric incorporation as indicated in Table 4.4.

Table 4.4: Change in water demand with fabric content

Fabric % (by volume)	W/C ratio
16	0.53
23	0.72
28	0.78

In fabric cement mixtures, other than the hydration reactions of cement, water is consumed for wetting fabric pieces due to water absorption and entrap water between woven yarns in the fabric. As a result, water demand of the mixture is increased with the increment of fabric incorporation.

Cast tile samples did not show a homogenous distribution of fabric pieces throughout the cement matrix. By visually observing the upper and bottom surfaces of the cast specimen, it was clearly identified that fabric pieces had moved to the upper surface during compaction due to its low density and in the meantime, cement paste had moved to the bottom layer as shown in Figure 4.5.

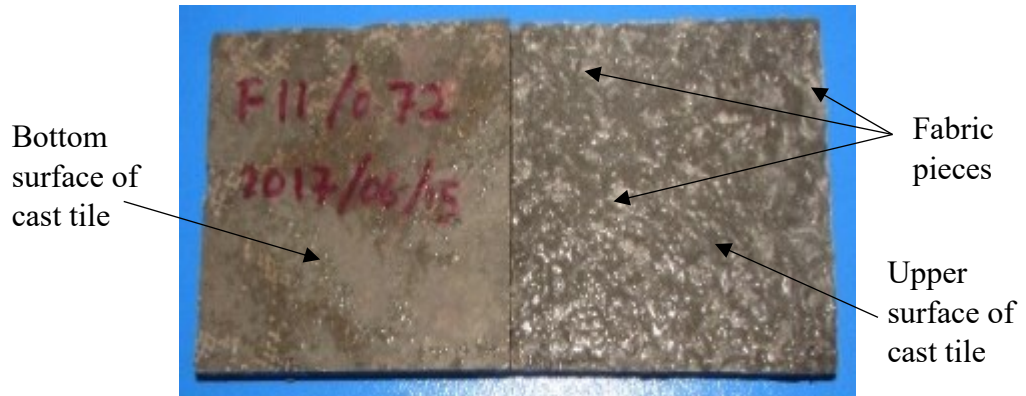


Figure 4.5: Surface texture of fabric cement composite

Variation in the surface texture of cast tile samples belonging to different mix proportions is shown in Figure 4.6. As it illustrates, surface porosity of the specimen increased with the increment of w/c ratio and the fabric content. Fines content of the composite reduced when the fabric content was increased as that resulted in high porosity. On the other hand, high w/c ratios increased the number of capillary pores which creates high porosity in the final product. In Figure 4.6, “FV” value indicates the fabric content by volume vs the water: cement ratio (two decimal values in Figure 4.6) of the mixture.

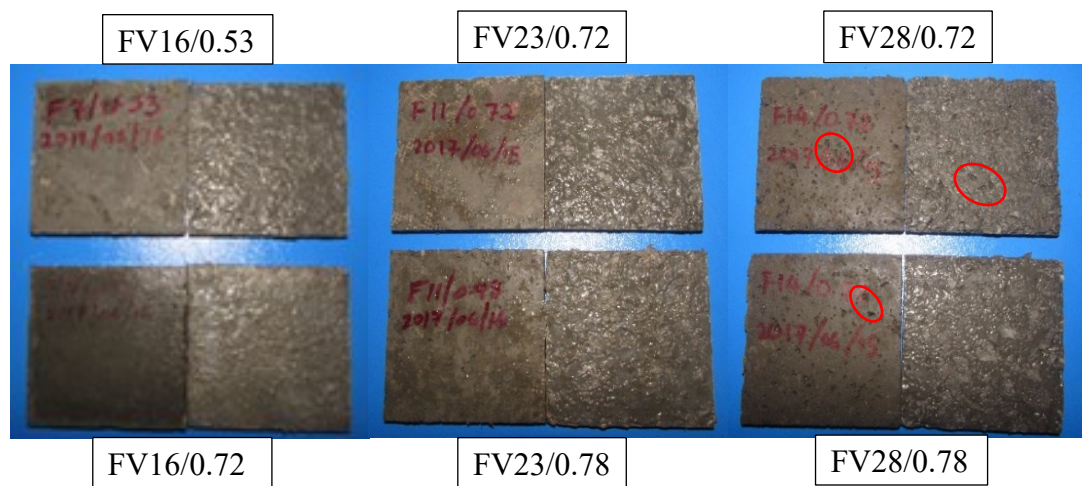


Figure 4.6: Surface texture of tile samples belonged to different mix proportions

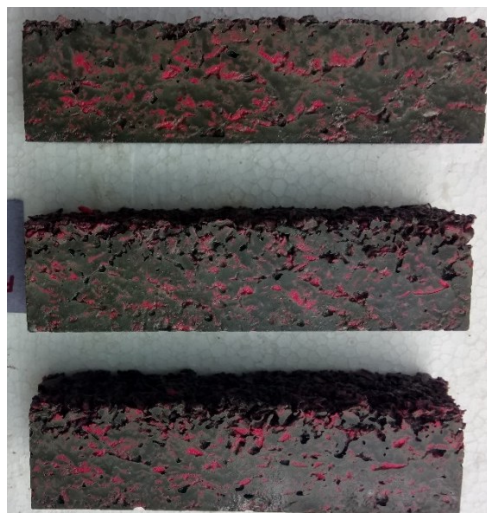
Prism samples were cast with the use of fabric cement mixture for further observations on fabric dispersion. Based on the cast orientation, the specimen's top surface, the bottom surface and side surface were observed for homogeneity as indicated in Figure 4.7. It shows that there is a high tendency to segregate fabric pieces from the cement paste due to the density difference.

Based on these observations it was decided to use viscosity modifying admixture to prevent segregation of fabric pieces from the cement matrix. The main purpose of using admixtures is to prepare a viscous cement slurry. Viscous mixtures lead to restrict the movement of fabric pieces in the cement matrix.



a) Top surface

b) Bottom surface



c) Side elevation

Figure 4.7: Surface texture of prism samples

4.7 Selection of suitable admixtures

Cement paste prism samples having the dimensions of 160 mm x 40 mm x 40 mm were cast without admixtures and with the use of two types of admixtures.

1. Cellulose-based viscosity modifier – Mecellose (Type C)
2. Polycarboxylic ether based superplasticizer – Hypercrete (Type H)

Cellulose-based viscosity modifier was used to prevent segregation of fabric pieces from the cement matrix while improving the homogeneity of the fabric cement composite. Polycarboxylic ether based superplasticizer was used to improve the workability at low w/c ratios.

Visual observations on the dispersion of fabric pieces throughout the specimen and water demand for mixtures were considered when selecting suitable admixtures for fabric cement composites. Figure 4.8 shows the dispersion of fabric pieces in the cement matrix along the side elevation and its cross-sections.

Based on the surface texture of cast specimens, fabric pieces can be clearly identified from the specimen cast without admixtures and specimen cast using type H admixture. Fabric pieces were properly coated with cement paste, with the use of type C admixture. This observation was mainly based on the modified viscosity of the fresh mixture. Accordingly, it illustrates that type C admixture helps to improve the homogeneity of the fabric cement composite while minimizing particle segregation.

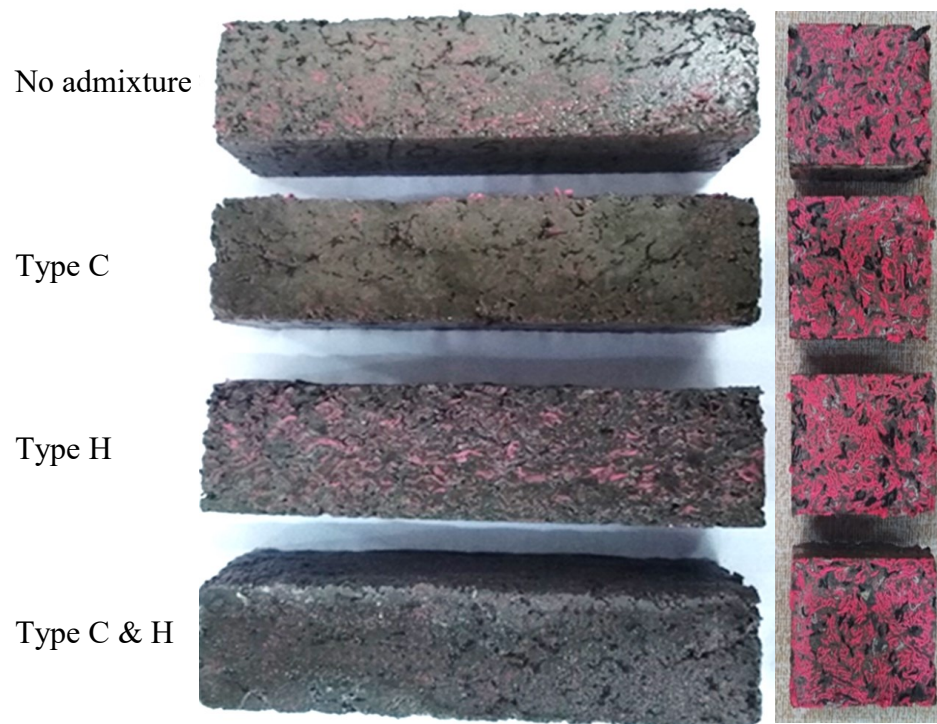


Figure 4.8: Variations in the dispersion of fabric pieces in prism samples

Type H admixture helps to reduce the water demand of the mixture to achieve the required workability to cast prism samples which leads to improve the strength of hardened product.

Considering the workability and homogeneity of fresh mixture, it was decided to use both type C and type H admixtures in casting fabric embedded cement-based products. The admixture dosage was decided based on admixture manufacturers' guidelines. Accordingly, it was decided to use type C admixture at 0.6% and 0.3% by weight of cement. Meanwhile, H type admixture was used at 1.2% and 0.6% by weight of cement. Considering the workability and homogeneity of the mixtures while focusing on the cost-effectiveness, it was decided to use type C admixture at 0.3% and type H admixture at 0.6% by weight of cement for fabric cement composites.

4.8 Flexural and compressive strength of cement paste prisms

Cement paste prism samples were cast by changing the fabric content to optimize the fabric incorporation into the cement matrix. Accordingly cast specimens were tested for flexural strength and compressive strength at 7 days and 28 days as per SLS ISO

679 [19]. Average strength results are tabulated in Table 4.5 and graphically presented in Figures 4.9 and 4.10.

Table 4.5: Flexural and compressive strength values of prisms cast by changing fabric incorporation

Mix ID	Fabric % by Volume	Flexural Strength (MPa)		Compressive Strength (MPa)	
		7 Days	28 Days	7 Days	28 Days
FV05/0.5/C,H	5	3.3	5.0	10.4	21.3
FV10/0.5/C,H	10	3.5	5.1	13.4	24.4
FV15/0.5/C,H	15	5.2	6.2	14.	25.3
FV20/0.5/C,H	20	6.6	8.4	15.7	27.3
FV25/0.5/C,H	2	7.4	11.6	15.1	29.7
FV26/0.5/C,H	26	8.2	12.4	14.9	27.2
FV28/0.5/C,H	28	5.9	12.3	14.9	25.5
FV30/0.5/C,H	30	4.8	9.8	12.2	21.3
FV35/0.5/C,H	35	4.3	7.7	6.1	10.3

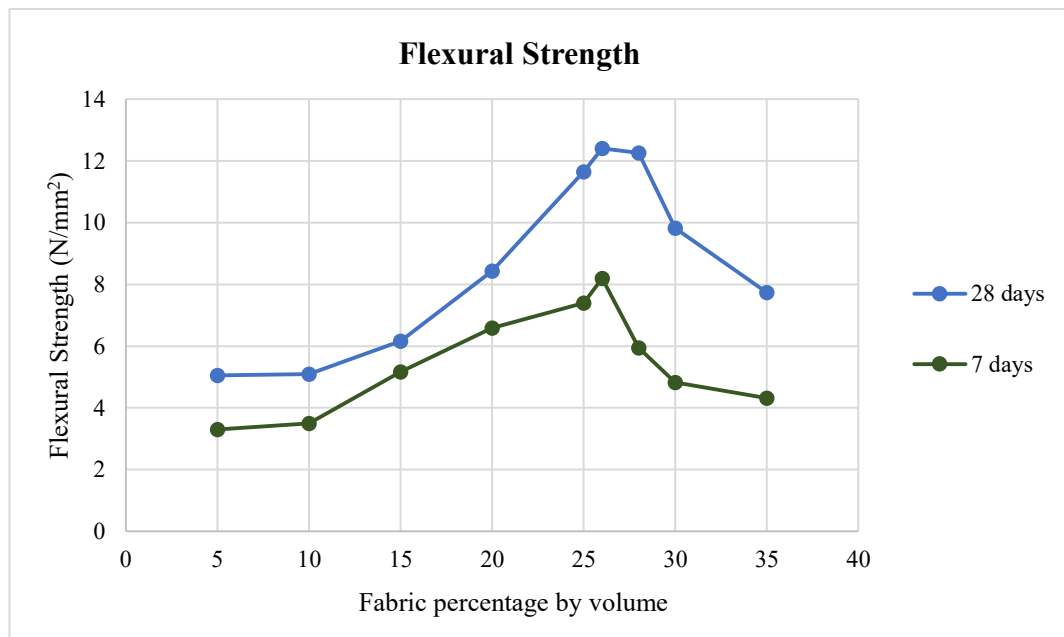


Figure 4.9: Flexural strength variation with fabric content

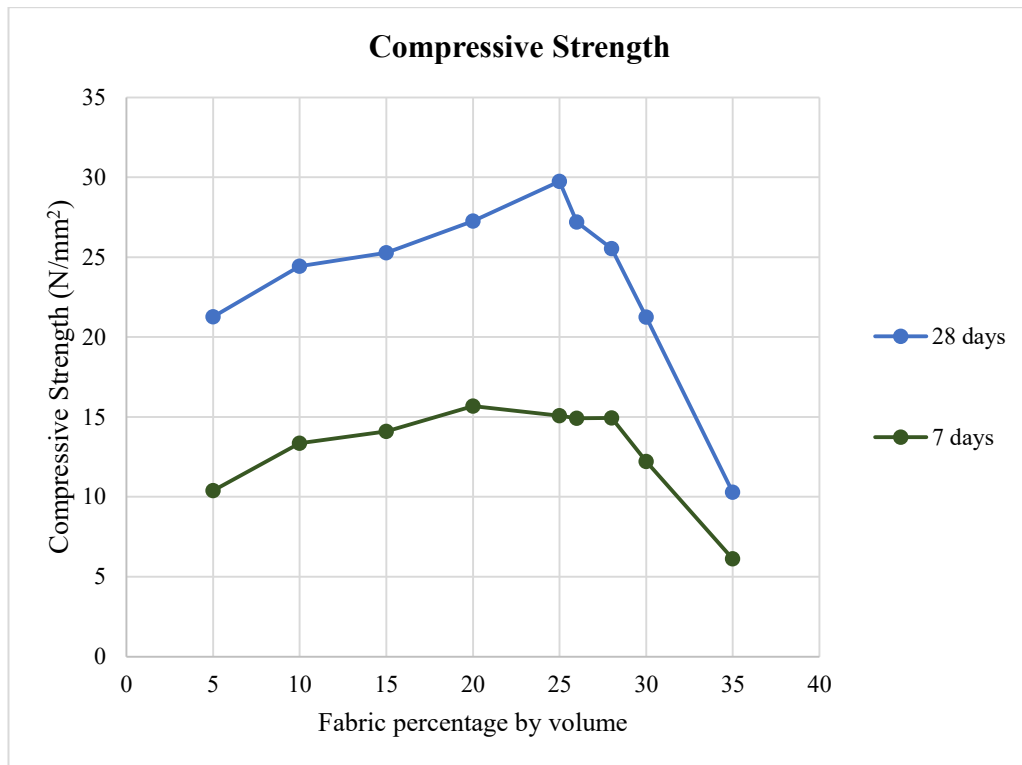


Figure 4.10: Compressive strength variation with fabric content

Under flexural strength, three specimens were tested for each mix proportion and for compressive strength six specimens were tested and average strength was considered in the analysis.

As shown in Figures 4.9 and 4.10, flexural strength and compressive strength gradually increased with the increase of fabric content up to 26% and 25% respectively. Afterward, strength decreased rapidly with the increase of fabric percentage. This behavior illustrates that fabric pieces act as reinforcing fibers in the cement matrix and optimum fiber effect was obtained at 26% of fabric content by volume. The fiber effect mainly affects the flexural strength rather than the compressive strength of the fabric cement composite. Further increment of fabric content (beyond 26%) leads to reduce the number of interconnecting bonds in the matrix as a result of the reduction in binder (cement) content. Based on the above strength results, fabric content that can be incorporated into the cement matrix to achieve the highest was 26% by volume. These observations were based on the cement paste prism samples cast using the shredded form of fabric pieces having a size less than 10 mm.

Cement paste prism samples were cast and tested for flexural strength and compressive strength with the use of fabric pieces belonged to different size segments for the selection of most suitable fabric size which gives the optimum reinforcing effect. Fabric pieces were categorized into different size segments through mechanical sieving using available sieve sizes. As a result of that, bandwidth of size segments were not equally distributed.

Previously found optimum fabric content of 26% by volume was used for the selection of suitable fabric size while maintaining w/c ratio at 0.5 with the use of C type and H type admixtures. The strength results obtained for the specimens cast with different sizes of fabric pieces were tabulated in Table 4.6 and graphically represented in Figures 4.11 and 4.12.

Table 4.6: Flexural and compressive strength results of prisms cast with different sizes of fabrics

Mix ID	Size segment of fabric pieces (mm)	Flexural Strength (MPa)	Compressive Strength (MPa)
F0-2/0.5/C,H	0-2.0	6.1	12.5
F2-3.5/0.5/C,H	2.0-3.5	11.0	21.8
F3.5-4/0.5/C,H	3.5-4.0	9.7	23.2
F4-5/0.5/C,H	4.0-5.0	12.7	22.1
F5-6.3/0.5/C,H	5.0-6.3	14.6	24.9
F6.3-8/0.5/C,H	6.3-8.0	14.8	23.3
F8-10/0.5/C,H	8.0-10	14.4	27.0
F10-12.5/0.5/C,H	10-12.5	13.9	28.7
F12.5-14/0.5/C,H	12.5-14	14.8	29.5

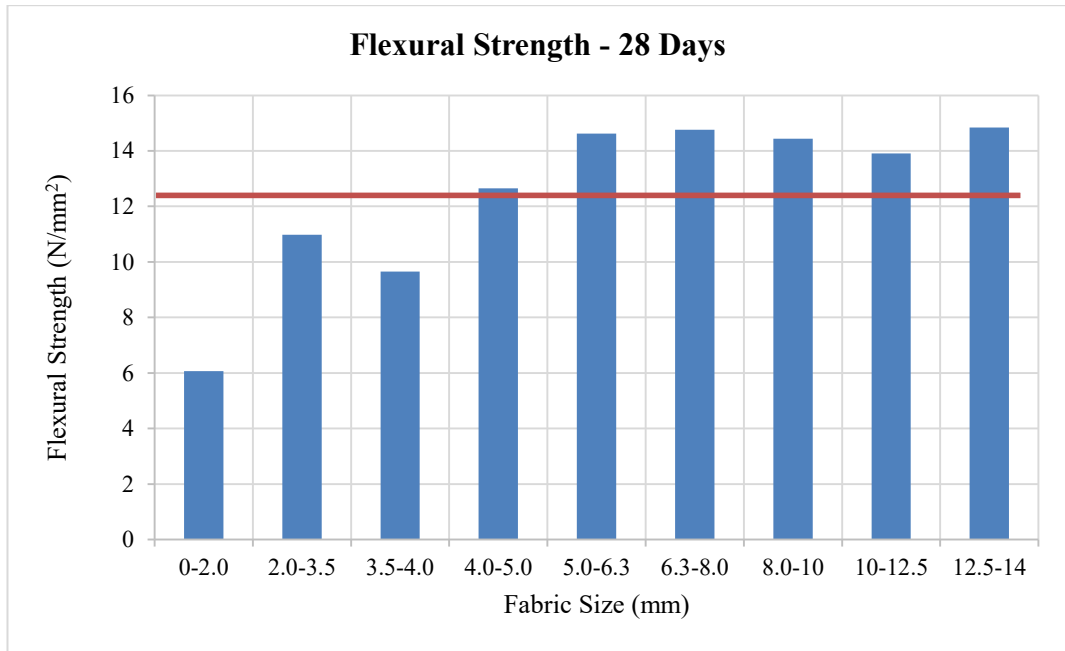


Figure 4.11: Flexural strength variation with size of fabric pieces

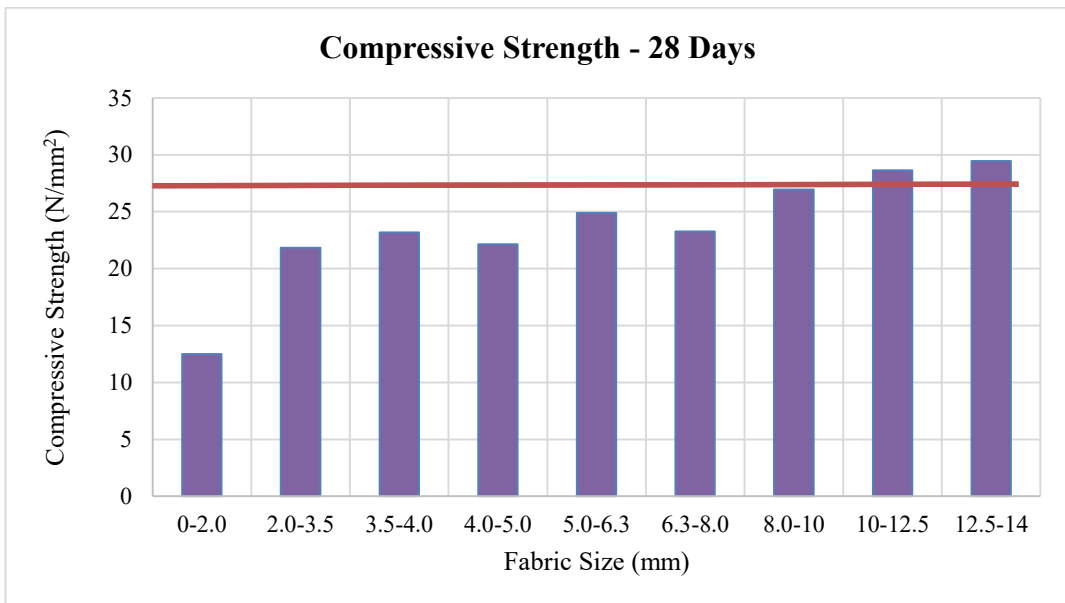


Figure 4.12: Compressive strength variation with size of fabric pieces

In Figures 4.11 and 4.12 red lines indicate the strength obtained for prism samples cast with mixed-size fabric pieces. Figures 4.11 and 4.12 show that strength slightly increased with the increment of the size of fabric pieces. When the size of fabric pieces increased beyond 5 mm, a considerable strength variation was not observed between different size segments.

The size distribution of fabric pieces in mixed size was analyzed under the sieve analysis test. As per the results of sieve analysis, 76% (by weight) of fabric pieces were smaller than 5 mm in size and 100% of fabric pieces were smaller than 10 mm in size. Specimens cast with mixed-size fabric, packing characteristics were improved due to the presence of fabric pieces belonging to different sizes which lead to minimize the voids in the composite. Shredding of fabric offcuts into a narrow size segment is very difficult and a uneconomical task. Considering these practical difficulties and insignificant variations in strength, it was decided to use the mixed size of fabric pieces in the range of 0 – 10 mm size for further experiments.

4.9 Failure pattern of fabric cement composites

Failure patterns obtained for fabric embedded cement paste prism samples were different from that of conventional cement-based mortar prisms. Under flexural load, fabric embedded prism specimens showed their ability to withstand further load through bending and propagation of the crack, without separating into pieces. It did not show a sudden failure point (brittle failure) as conventional cement-based products. Figure 4.13 illustrates the failure pattern obtained under flexural test. Specimens tested for flexural strength were used for compressive strength test, therefore it was required later to break these specimens manually into two pieces.



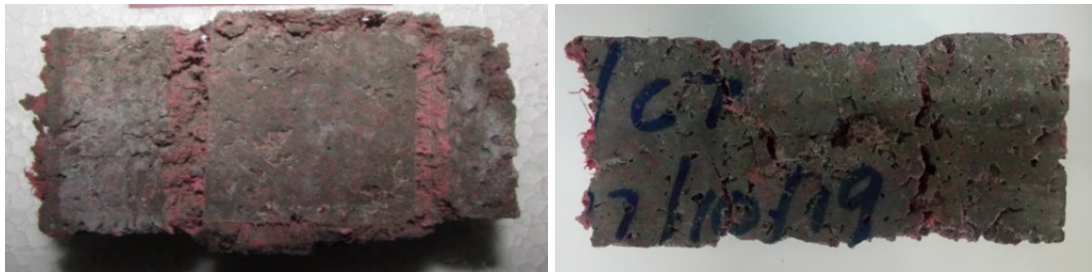
Figure 4.13: Failure pattern under flexural load



Figure 4.14: Fracture surface under flexural load

Under flexural load, failure pattern of the specimen was identified as a ductile failure. Visual observations on fracture surface (Figure 4.14) illustrate that the final failure was due to the removal of interconnecting bonds between fabric pieces and cement matrix. As a result of that, partially removed fabric pieces can be clearly identified from the fracture surface. Accordingly, this failure pattern is an evidence for the fiber effect of fabric pieces in the cement matrix.

Fabric cement composite has the ability to withstand higher compression loads while creating a plastic deformation as shown in Figure 4.15. When conventional cement-based products are subjected to compression loads, at the failure point they will separate into a numerous pieces showing a brittle failure. Hence, the ductile failure pattern obtained for fabric cement composite indicates its energy absorption capability.



a) Top surface

b) Side view

Figure 4.15: Failure pattern under compression load

4.10 Surface texture of fabric embedded paving blocks

Paving block samples were cast with 26% (by volume) shredded fabric (size less than 10 mm), cement and manufactured sand. In this process, fabric is considered as the reinforcing fiber, cement as bonding agent and manufactured sand as a filler material.

Mix proportions for the casting of paving blocks were changed by reducing the binder content while increasing the sand content as indicated in Table 4.7 to select a suitable mixture.

Table 4.7: Mix proportions used for casting of paving blocks

Mix ID	Constituents percentage by volume %			W/C
	Fabric	Cement	Manufactured sand	
FV26/MS05/0.5/C,H	26	69	5	0.5
FV26/MS10/0.5/C,H	26	64	10	0.5
FV26/MS15/0.6/C,H	26	59	15	0.6
FV26/MS20/0.6/C,H	26	54	20	0.6
FV26/MS25/0.6/C,H	26	49	25	0.6
FV26/MS30/0.6/C,H	26	44	30	0.6
FV26/MS35/0.7/C,H	26	39	35	0.7
FV26/MS40/0.8/C,H	26	34	40	0.8
FV26/MS45/0.8/C,H	26	29	45	0.8
FV26/MS50/1.0/C,H	26	24	50	1
FV26/MS55/1.3/C,H	26	19	55	1.3
FV26/MS60/1.6/C,H	26	14	60	1.6



Figure 4.16: Surface texture of paving blocks belonged to different mix proportions

Fabric content was kept as constant at 26% by volume for the casting of paving blocks shown in Figure 4.16, but it seems that the appearance of fabric pieces on the surface increased with the increment of sand content. Binder content in the mixture gradually decreased with the increment of sand content, as a result of that available cement paste was not sufficient to coat the fabric pieces. Therefore, the appearance of fabric pieces gradually increased due to the reduction of cement content in the mixture.

4.11 Compressive strength of paving blocks

Cast paving blocks with different mix proportions were tested for compressive strength according to the method described in SLS 1425 Part 2 [20]. At the initial stage of compressive loading, paving blocks showed an elastic deformation. With the increase of compressive load, deformation of paving blocks changed from elastic to plastic deformation as shown in Figure 4.17 which resulted in permanent deformation. As a result of that, it is not possible to identify a peak load as a failure point for the calculation of compressive strength. Based on the load-deformation pattern obtained for paving blocks, it is possible to identify a changing point from the elastic deformation region to the plastic deformation region for the calculation of compressive strength (Figure 4.17).

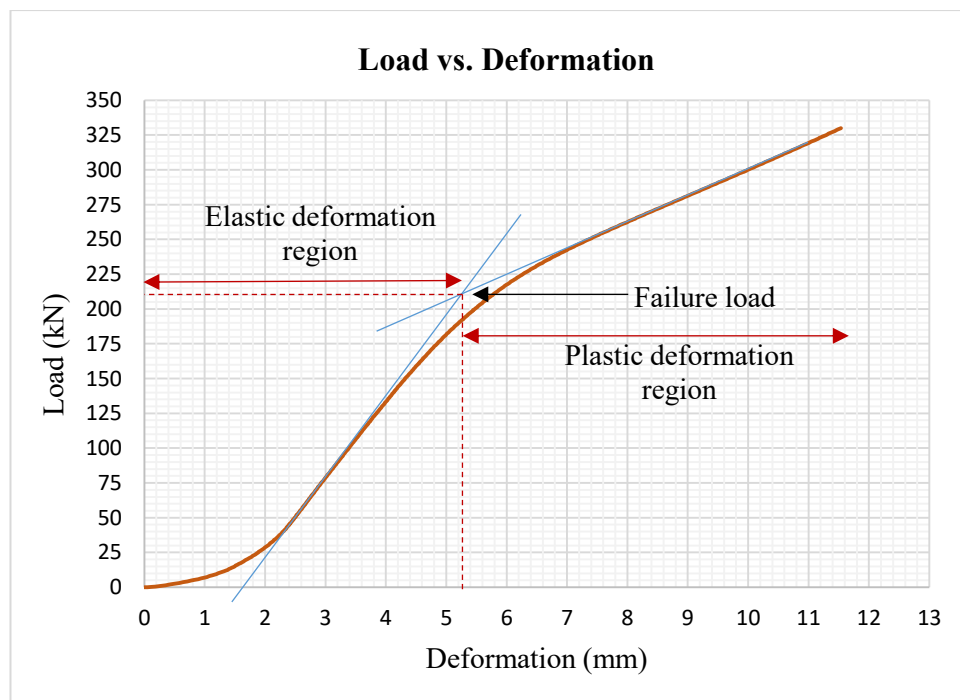


Figure 4.17: Load deformation pattern of paving block under compression load

The compression load belonging to the plastic deformation range changes the sharpness of the edges of the paving block while increasing the plan area of the block as shown in Figure 4.19. When these blocks were practically applied for pavement structure, this kind of plastic deformation was restricted by adjacent paving blocks. Accordingly, under confined conditions in a paved surface, fabric embedded paving blocks have the ability to withstand higher loads than the results indicated under unconfined compressive strength.

Table 4.8: Compressive strength results of fabric embedded paving blocks

Mix ID	Compressive Strength (MPa)	Failure Strain (%)
FV26/MS05/0.5/C,H	25.21	4.67
FV26/MS10/0.5/C,H	22.22	5.33
FV26/MS15/0.6/C,H	17.87	5.50
FV26/MS20/0.6/C,H	17.42	5.17
FV26/MS25/0.6/C,H	13.52	5.17
FV26/MS30/0.6/C,H	7.62	5.50
FV26/MS35/0.7/C,H	6.00	7.00
FV26/MS40/0.8/C,H	2.63	6.67
FV26/MS45/0.8/C,H	1.92	5.00
FV26/MS50/1.0/C,H	1.42	5.83
FV26/MS55/1.3/C,H	0.74	5.50
FV26/MS60/1.6/C,H	0.12	0.33

Compressive strength results indicated in Table 4.8 are average values obtained by testing three nos. of specimens belonging to each mix proportion.

As specified in SLS 1425 Part 1: [Specification for concrete paving blocks, Part 1: Requirements] [27] minimum compressive strength requirement for 60 mm thick paving block for pedestrian use is 15 N/mm². Accordingly, “FV26/MS20/0.6/C,H” mixture satisfied the compressive strength requirement at low material cost due to reduction of cement content in the mixture. Paving block did not show any physical damage (crack initiation or any kind of plastic deformation) at the reported strength values, since elastic to plastic deformation point used for identification of failure load. The compression load applied for the specimen shown in Figure 4.19 is approximately 50% higher than the failure load considered for strength calculation.

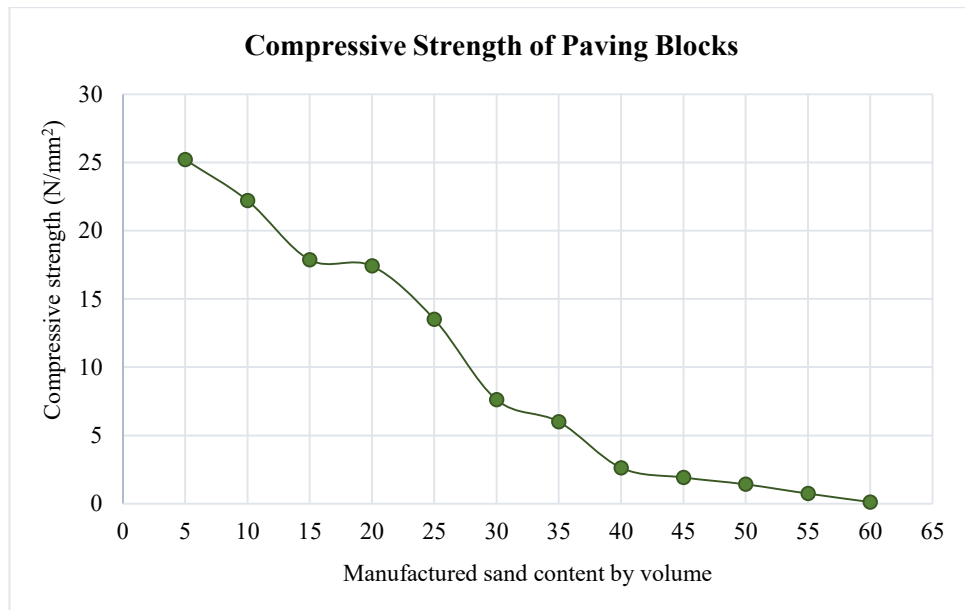


Figure 4.20: Compressive strength variation of paving blocks

As illustrated in Figure 4.20, compressive strength gradually decreased with the increment of sand content. The binder content of the mixture proportionally decreased with the increment of sand content. As a result, number of interconnecting bonds in the structure gradually decreased which resulted in decreasing the compressive strength of the fabric embedded paving block. Failure pattern obtained for fabric embedded paving block gradually changed from ductile failure pattern to brittle failure pattern with the reduction of binder content in the mixture.

4.12 Tensile splitting strength

Paving blocks belonging to different mix proportions were tested for tensile splitting strength as per the method described in BSEN 1338: [Concrete paving blocks- Requirements and test methods] [21] to select the suitable mixture for fabric embedded paving blocks based on flexural properties.

According to the test procedure specified in BSEN 1338, the compression load was applied to the test specimen through a rigid spherical surface with 75 mm radius, from both the top and bottom surfaces of the specimen until failure as shown in Figure 4.21.

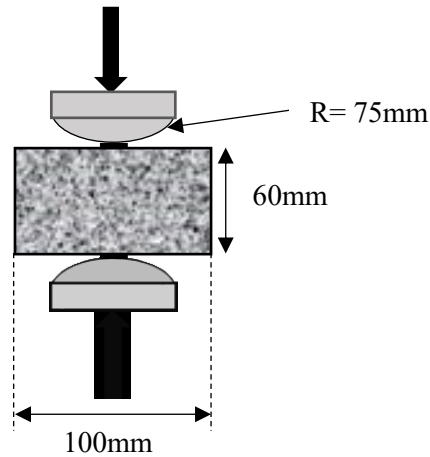


Figure 4.21: Loading arrangement of tensile splitting strength test

In practical applications, paving blocks were mainly subjected to flexural loads, rather than compression loads due to the footprint of passengers and movement of vehicles. The shredded fabric used in the paving block is the main contributor to the improvement in tensile splitting strength.

Table 4.9: Tensile splitting strength of fabric embedded paving blocks

Mix ID	Tensile Splitting Strength (MPa)	Failure Strain (%)
FV26/MS05/0.5/C,H	5.56	16.69
FV26/MS10/0.5/C,H	5.38	17.65
FV26/MS15/0.6/C,H	4.75	16.68
FV26/MS20/0.6/C,H	4.18	19.56
FV26/MS25/0.6/C,H	4.21	17.30
FV26/MS30/0.6/C,H	3.64	44.06
FV26/MS35/0.7/C,H	2.90	46.98
FV26/MS40/0.8/C,H	2.95	47.62
FV26/MS45/0.8/C,H	1.42	48.29
FV26/MS50/1.0/C,H	1.08	52.06
FV26/MS55/1.3/C,H	0.72	47.17

Tensile splitting strength results of different mix proportions are tabulated in Table 4.9 and these average strength values were obtained by considering two individual test results for each mix proportion.

The minimum standard requirement for Tensile splitting strength is 3.6 MPa as specified in BSEN 1338: [Concrete paving blocks- Requirements and test methods] [21]. Accordingly “FV26/MS30/0.6/C,H” mixture can be selected for the casting of fabric embedded paving blocks considering flexural properties at reduced material cost.

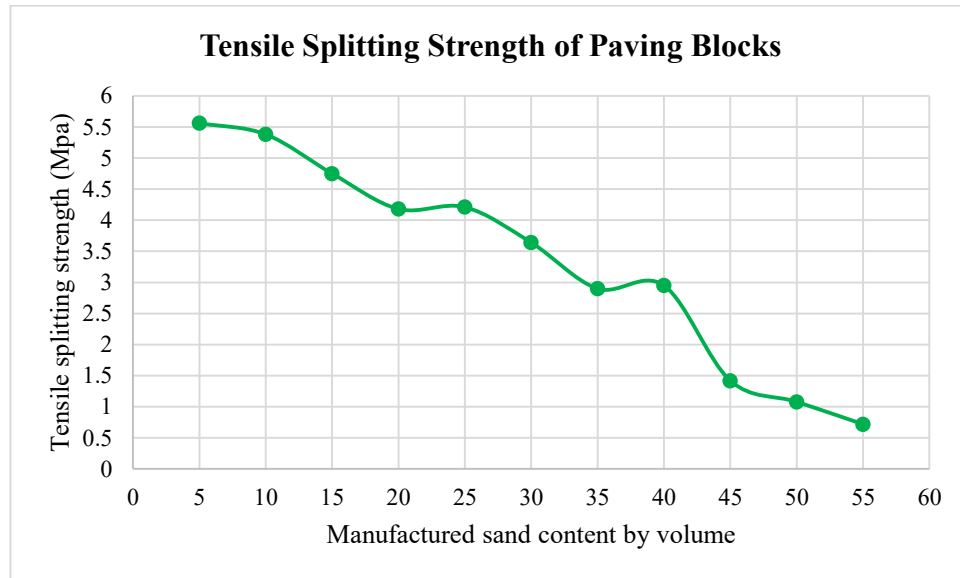
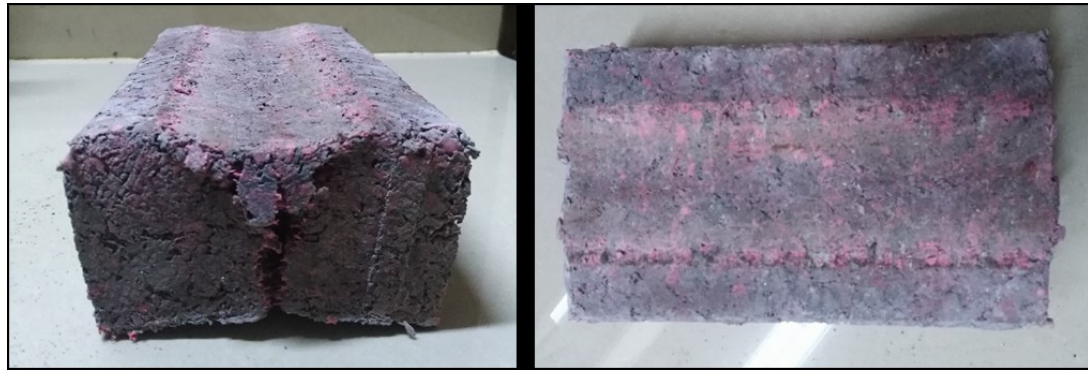


Figure 4.22: Tensile splitting strength variation of paving blocks

As illustrated in Figure 4.22, the tensile splitting strength of paving blocks gradually decreased with the increment of sand content. Cement content in the mixture gradually reduced with the increment of sand content. Then the number of inter-connecting bonds was proportionally reduced due to the reduction of binder content in the mixture. As a result of that internal bonds become weaker, the strength of paving blocks decreased while increasing the failure strain of the specimen. Increment of failure strain leads to change its failure pattern from ductile mode to brittle mode.

Failure patterns obtained under tensile splitting strength of paving blocks are shown in Figure 4.23. When load was applied to the test specimen at a constant rate, initially the specimen was subjected to elastic deformation and then, to plastic deformation. Thereafter, a crack was initiated and propagated through the centerline of the paving block indicating the failure of the test specimen.



a) Side view

b) Top surface

Figure 4.23: Failure pattern of paving block under tensile splitting test

Based on compressive strength and flexural strength test results, three mix proportions were selected for the casting of paving blocks to evaluate abrasion resistance, skid resistance, permeability, shock absorption capability and durability were for selected mixtures. Details of mix proportions of the selected mixtures are tabulated in Table 4.10. FV26/MS20/0.6/C,H mixture was selected due to satisfied compressive strength under least cost of materials. Then FV26/MS30/0.6/C,H mixture was selected considering the satisfaction of tensile splitting strength requirement under least cost of materials. FV26/MS25/0.6/C,H mixture was considered for further tests based on its material composition which lies in between the above mentioned two selected mixtures.

Table 4.10: Selected mix proportions for the casting of paving blocks

Mix ID	Constituents percentage by volume %			W/C	Admixture % by weight of cement	
	Fabric	Cement	Manufactured sand		Type C	Type H
FV26/MS20/0.6/C,H	26	54	20	0.6	0.3	0.6
FV26/MS25/0.6/C,H	26	49	25	0.6	0.3	0.6
FV26/MS30/0.6/C,H	26	44	30	0.6	0.3	0.6

The compaction of the fresh mixture in the mould was further improved by using a standard metal tamping rod which is prescribed for the slump test of concrete. Specimens were cast according to selected mix proportions and were tested for all parameters including compressive strength and tensile splitting strength to identify the

improvements in compaction when compared with the use of 2”×2”×6” timber rod for tamping.

The strength results obtained for specimens cast with improved compaction are tabulated in Table 4.11 and graphically represented in Figure 4.24.

Table 4.11: Strength results of selected paving block mixtures

MIX ID	Compression Test		Tensile Splitting Test	
	Compressive Strength (MPa)	Failure Strain (%)	Splitting Tensile Strength (MPa)	Failure Strain (%)
FV26/MS20/0.6/C,H	20.83	7.81	5.6	23.49
FV26/MS25/0.6/C,H	18.17	7.73	5.4	23.27
FV26/MS30/0.6/C,H	11.25	8.42	3.8	30.78

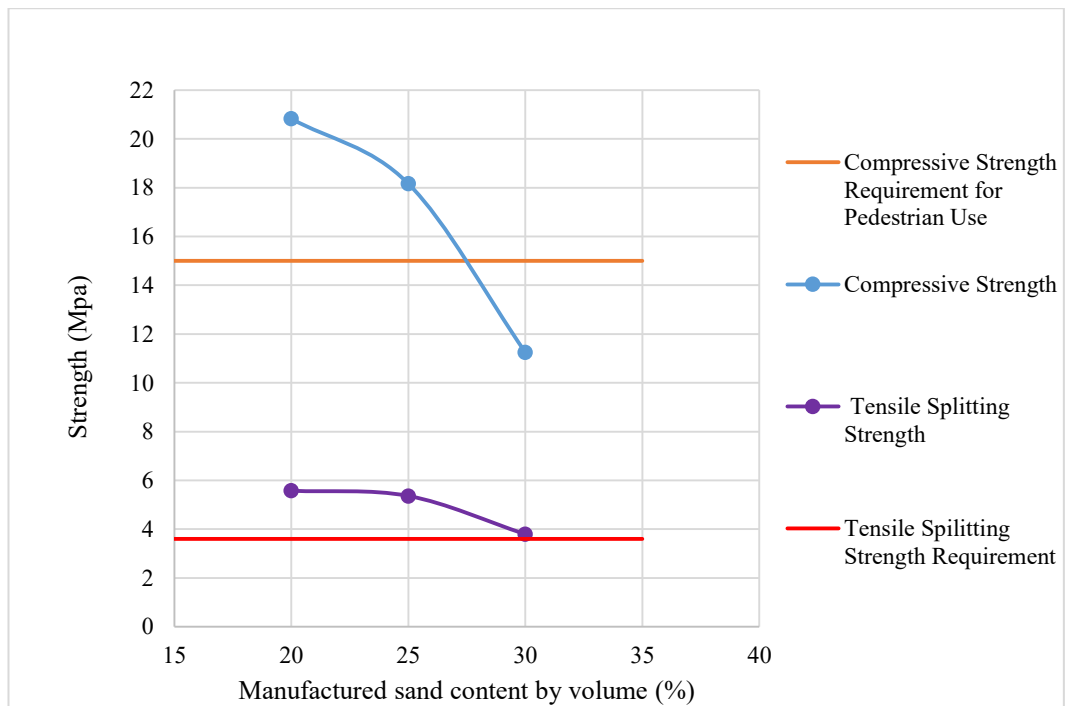


Figure 4.24: Strength variation of selected paving block mixtures

The above strength results illustrate that improvement in compaction greatly enhances the mechanical properties in the final product due to improved bonding characteristics.

Paving blocks cast according to “FV26/MS25/0.6/C,H” mixture satisfies compressive strength requirement for pedestrian use and tensile splitting strength requirement for all kinds of pavement structures. Therefore “FV26/MS25/0.6/C,H” mixture and two mixtures close to the mix FV26/MS25/0.6/C,H were tested for abrasion resistance, skid resistance, water infiltration capability, shock absorption capability and durability to select the most suitable mix for paving blocks.

4.13 Abrasion resistance

Abrasion resistance test was performed to assess the wearing resistance of fabric embedded paving blocks while identifying the tendency for releasing fabric pieces from the paving block.

Results obtained for abrasion resistance of fabric embedded paving blocks are tabulated in Table 4.12.

Table 4.12: Abrasion resistance test results

MIX ID	Abrasion Resistance (mm)	
	Measured Abrasion Value	Standard Requirement [21]
FV26/MS20/0.6/C,H	17	≤ 20
FV26/MS25/0.6/C,H	17	
FV26/MS30/0.6/C,H	18	

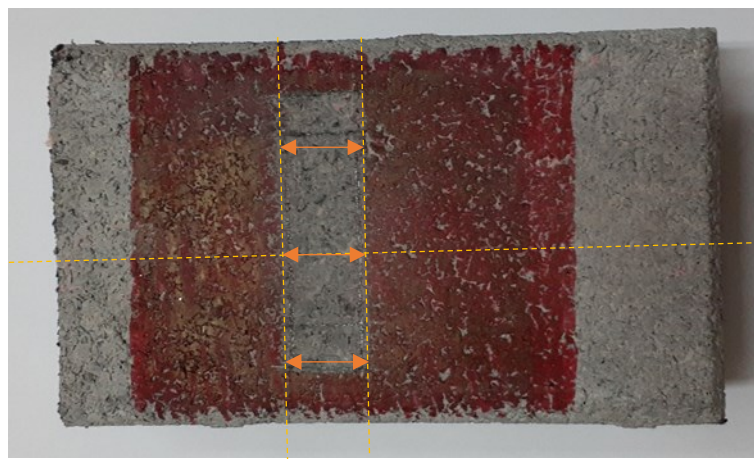


Figure 4.25: Specimen subjected to the abrasion resistance test

Figure 4.25 illustrates the methodology used to take the measurements for the determination of the abrasion resistance value. Abrasion resistance test results

obtained for selected mix proportions fulfilled the standard requirement as per BSEN 1338 [21]. Other than that abraded surface (see Figure 4.25) of fabric embedded paving blocks did not show the tendency for fully or partially removal of fabric pieces from the paving block.

4.14 Skid resistance

Skid resistance of paving blocks was measured as Unpolished Slip Resistance Value (USRV) with the use of pendulum friction test equipment. The test was performed according to the method described in BSEN 1338: [Concrete paving blocks- Requirements and test methods] [21]. The test was performed on four numbers of specimens corresponding to each mix proportion at the saturated condition. Test specimens in wet conditions were used for the test to observe its minimum skid resistance value. Skid resistance test results of selected mix proportions are indicated in Table 4.13.

Table 4.13: Skid resistance test results

MIX ID	Skid Resistance (USRV)	
	Measured Value	Standard Requirement [27]
FV26/MS20/0.6/C,H	80	≥ 55
FV26/MS25/0.6/C,H	80	
FV26/MS30/0.6/C,H	80	

Skid resistance test is used to evaluate the surfaces of pavements, as inadequate skid resistance cause accidents. USRV represents the frictional properties on the upper face of the paving blocks. It is very useful to get an idea about the safe movements of users on the surface of paving blocks based on its slippery characteristics. USRV obtained for selected mix proportions of fabric embedded paving blocks is considerably higher than the standard requirement for all kind of pavement structures as per SLS 1425-1 [27]. Accordingly, skid resistance of fabric embedded paving blocks can be considered at a safe level in the absence of foreign materials on the surface. Such foreign materials are grease, oil, etc may affect the frictional properties of the surface.

4.15 Permeability

Permeability characteristics of product or structure mainly depend on its porosity, size of pores and connectivity of pores. In cement-based applications, it highly depends on the w/c ratio of the mixture and entrapped air during casting which is normally depends on compaction in the absence of special materials like air entraining admixtures.

Water percolation capacity of fabric embedded paving blocks was measured with the use of core samples extracted from cast paving blocks while applying 1.1 bar constant pressure head. The amount of water percolate through the specimen was measured at constant time intervals and test results are tabulated in Table 4.14 and graphically represented in Figure 4.26.

Table 4.14: Permeability test results

Sample ID	Percolated Water (liters/m ²)			
	30 minutes	60 minutes	90 minutes	120 minutes
F26/MS25/0.6/C,H	99.6	205.9	321.3	440.1
F26/MS30/0.6/C,H	88.2	176.5	270.4	363.2
Conventional paving block	1.1	2.0	2.7	3.2

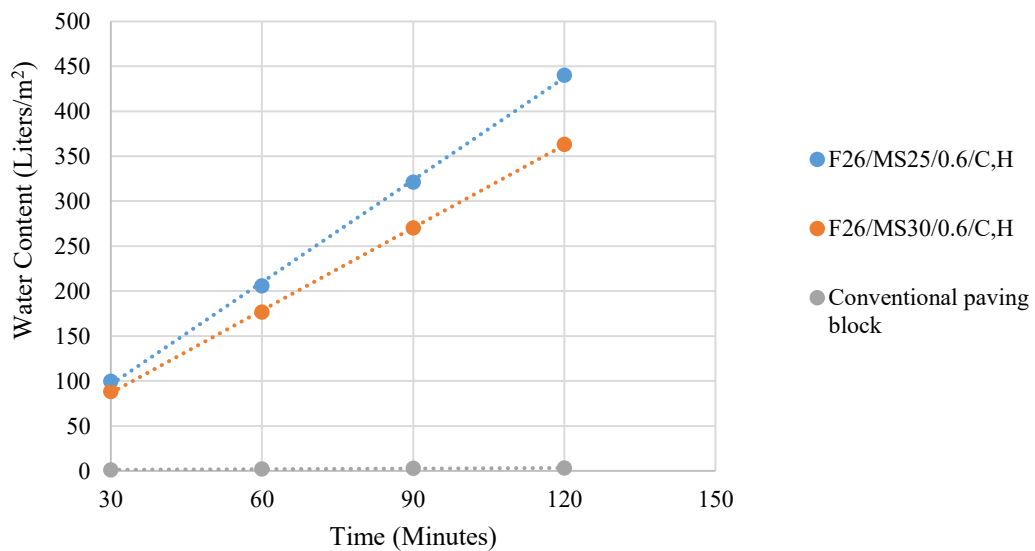


Figure 4.26: Variation of water permeability in different mixtures

According to the Darcy's law, water permeability of a porous structure is proportional to the flow rate of a homogeneous fluid at constant pressure difference [28]. Accordingly, test results indicated in Table 4.14 illustrates that water infiltration capability of fabric embedded paving block is approximately 100 times higher than that of conventional concrete paving blocks.

In fabric embedded paving blocks, small fabric pieces facilitate the path for movement of water through void spaces in between woven yarns and by wetting yarns while facilitating moisture movements to nearby spaces.

Water demand for fabric-sand-cement mixture is comparatively high when compared with sand-cement mixture due to the water entrapment in fabric pieces. It is due to the higher w/c ratio of fabric embedded paving block than that of the conventional concrete paving block. The w/c ratio used for casting fabric embedded paving block is 0.6, which is considerably higher than the water required for 100% hydration of cement. Use of high w/c ratio leads to increase the number of capillary pores in the hydrated product. The number of interconnected pores in the hydrated product directly affects the water permeability of cast specimens. Increase of porosity in constant volume leads to an increase in the number of interconnected pores that facilitate the path for movement of water which increases the water percolation capacity.

Improved water permeability of fabric embedded paving blocks is very useful to reduce surface runoff during heavy rains and prevent flash flooding. It is an environmentally friendly property that helps to recharge the underground water table while reducing soil erosion.

4.16 Shock absorption

Shock absorption of fabric embedded paving blocks was analyzed by measuring its force reduction capability as described in section 3.4.7. Test results of each mix proportion and force reduction percentages were indicated in Table 4.15.

Table 4.15: Shock absorption test results

Sample ID	Maximum Impact Force (N)	Average Value of Maximum Impact Force (N)	Force Reduction Percentage (%)
F26/MS25/0.6/C,H	9348	9322	21.44
	9522		
	9423		
	8993		
F26/MS25/0.6/C,H	9624	9382	20.93
	9009		
	9616		
	9277		
F26/MS30/0.6/C,H	9537	9414	20.66
	9017		
	9470		
	9632		
Concrete	12546	11866	0
	11576		
	11568		
	11773		

According to the test results indicated in Table 4.15, the force reduction capability of fabric embedded paving blocks is about 20%. It illustrates that under the application of the same impact load, the pavement of fabric embedded paving blocks has the ability to reduce its sensible force by 20% when compared with concrete pavement. This feature can be expressed as its shock absorption capability.

Improved shock absorption capability is beneficial for its end users. When this kind of paving blocks are used for footpaths, it will facilitate better foot comfort for pedestrians due to the force absorbance of foot stroke. Conventional concrete pavement is a kind of rigid pavement, but fabric embedded cement based blocks paved pavements are more close to flexible pavements due to flexibility and elasticity characteristics of polyester-spandex fabric pieces.

Shock absorption capability is a standard requirement for artificial sports surfaces as specified in BSEN 15330-1: [Surfaces for sports areas - Synthetic turf and needle punched surfaces primarily designed for outdoor use; Part 1- Specification for synthetic turf surfaces for football, hockey, rugby union training, tennis and multi-sports use] [29]. Accordingly, fabric embedded paving blocks satisfied the standard

requirement for tennis surfaces under shock absorption class 1, in which force reduction percentage should be in the range of 15% to 24%.

Figure 4.27 illustrates how the force reduction capability of sports surfaces benefit athletes.



Figure 4.27: Use of force reduction capability to the benefit of athletes [30]

Other than the factors described in Figure 4.27 it helps to reduce long term impact injuries of athletes and reduce physical damages during accidents. According to the above explanations, force reduction is useful to sports surfaces in two ways as facilitating player comfort while preventing injuries.

4.17 Durability

4.17.1 Durability under moist and temperature conditions

Durability evaluation results of fabric embedded paving blocks and concrete paving blocks under moist and temperature conditions were tabulated in Table 4.16.

Table 4.16: Durability evaluation results under moist and temperature conditions

Mix ID	Average Tensile Splitting Strength Ratio	Standard Deviation	Soak-dry Performance Criteria ≥ 0.75
FV26/MS20/0.6/C,H	0.907891	0.018561	0.897
FV26/MS25/0.6/C,H	0.834891	0.058701	0.801
FV26/MS30/0.6/C,H	0.827058	0.073442	0.784
Concrete paving block	0.923039	0.073360	0.880

According to the test results indicated in Table 4.16, durability of fabric embedded paving blocks is at a satisfactory level considering the requirements specified in the ISO 8336 standard [25]. Other than that, strength reduction of concrete paving blocks were evaluated for comparison purpose. According to test results, strength reduction of fabric embedded paving blocks is in the same range of strength reduction corresponding to conventional concrete paving blocks. Therefore, deterioration of fabric embedded paving blocks under moisture conditions was not at an inferior level when compared with conventional paving blocks.

During the drying cycles (keeping the fabric embedded paving blocks and concrete paving blocks in the oven at 60⁰C for 6 hours) it was observed that surface temperature of fabric embedded paving blocks is considerably lower than that of the conventional concrete paving block. Pervious nature of fabric embedded paving blocks is the main factor for this effect. Porous structure provides insulation effect against rapid heat transfer by conduction [31]. Additionally, pervious nature can provide evaporative cooling when water is present in the system [31]. This effect may reduce the possibility of heating pavement structures by sunlight and in addition, facilitate better foot comfort.

4.18 Cost calculation for fabric embedded paving block

Manufacturing cost mainly depends on the production scale. In calculation of production cost, it is required to consider energy consumption, machine wearing, labour cost and material cost. Out of these cost factors material cost is remained as constant and does not depend on the scale of production. Therefore material cost for the selected mixtures of fabric embedded paving block was calculated as follows.

Material cost calculation was carried out for casting of blocks with following dimensions (see Figure 4.28).

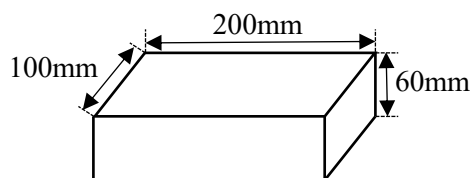


Figure 4.29: Dimensions of paving block

Figure 4.30: Dimensions of paving block

Table 4.17: Material cost for fabric embedded paving block

Mix ID	Type of Material	Required Material Quantity per Block	Material Cost (LKR)	Material Cost per Block (LKR)
F26/M20/0.6/C,H	Cement	1115g	22.85	32.10
	Shredded fabric	226g	0.00	
	Manufactured sand	340g	2.00	
	Mecellose	3.3g	3.95	
	Hypercrete	6.6ml	3.30	
F26/M25/0.6/C,H	Cement	1015g	20.80	29.90
	Shredded fabric	226g	0.00	
	Manufactured sand	425g	2.50	
	Mecellose	3g	3.60	
	Hypercrete	6ml	3.00	
F26/M30/0.6/C,H	Cement	910g	18.65	27.6
	Shredded fabric	226g	0.00	
	Manufactured sand	515g	3.00	
	Mecellose	2.7g	3.25	
	Hypercrete	5.4ml	2.70	

Based on the performance, F26/M20/0.6/C,H and F26/M25/0.6/C,H mixtures are suitable for paving blocks. Then material cost was considered for the selected mixture based on performance. Hence F26/M25/0.6/C,H mixture is selected for fabric embedded paving blocks considering the satisfactory performance and material cost.

Cement consumption of fabric embedded paving block is comparatively higher than that of conventional concrete paving blocks. Therefore material cost of this product is relatively high value. But this cost increment cannot be considered as a disadvantage due to the availability of special features (shock absorption and permeability) in this product.

5 CONCLUSIONS

Synthetic fiber blended fabric waste is difficult to recycle due presence of synthetic fiber blend. Therefore, at present it is considered as a problematic waste. Polyester spandex is a kind of commonly used synthetic fiber blended fabric in apparel industry which consist of polyester and spandex fiber blend. In this study, utilization of this waste as a raw material to produce paving blocks was investigated.

It was found that spandex fiber blended fabric waste in shredded form can be used as reinforcement in the cement-based composites with the use of viscosity modifying admixture (cellulose based viscosity modifier) and a superplasticizer (poly-carboxylic ether based superplasticizer). Viscosity modifier was used to prevent segregation of fabric pieces from the cement paste due to its density difference. Since the water demand of fabric – cement mixture was relatively high due to entrapped water in woven fabric pieces, superplasticizer was used to improve the workability of mixture at low water/cement ratios (0.5-0.6).

Mixed size shredded fabric pieces in the range of 0 - 10 mm gave better reinforcing effect with improved packing characteristics. Optimum reinforcing effect was observed at 26% (v/v) of fabric content in fabric – cement composite.

Based on the findings of the preliminary investigation with cement paste and fabric mixture, fabric embedded paving bocks were developed to comply with the standard requirements specified in SLS 1425 and BSEN 1338. Most suitable mixture for casting of polyester spandex fabric embedded paving blocks was found to be 26% of shredded fabric, 25% of fine aggregate and 49% of cement by volume at 0.6 water/cement ratio together with the use of viscosity modifier (Mecellose) and a superplasticizer (Hypercrete) at a dosage of 0.3% and 0.6% by weight of cement respectively.

The tensile splitting strength of selected mixture of fabric incorporated paving blocks was 5.4 MPa. Meanwhile, abrasion resistance and skid resistance of blocks were 17 mm and 80 USRV, respectively. The above-mentioned mixture satisfied the standard requirements specified in BSEN 1338. Further, the compressive strength of fabric embedded paving blocks was 18 MPa, which satisfies the requirements specified for pedestrian use (≥ 15 MPa) in SLS 1425: Part 1.

Under compression load, fabric embedded paving block is initially subjected to elastic deformation and thereafter plastic deformation, while reducing its thickness and expanding surface area. This ductile failure pattern indicates its energy absorption capability. Therefore, its shock absorption capability was determined as per BSEN 14808. It was found that the developed paving blocks have the capability to reduce impact force by 20%. Thus, the fabric embedded paving blocks can be recommended for outdoor sports surfaces which satisfies the requirements for tennis surfaces as specified in BSEN 15330-1.

The water infiltration capability of the fabric embedded paving blocks was found to be 100 times higher than that of conventional concrete paving blocks. The high water infiltration property of the developed paving blocks facilitates reduction of surface runoff of rainwater when it is used for paving of lightly loaded areas such as foot paths.

Accordingly, aforementioned mixture is a suitable formula for manufacturing paving blocks for outdoor sports surfaces, foot paths and similar applications.

Recommendations for Future Work

- Investigation of utilizing a mixture of ultra-fine crush rock particles, fly ash and cement as the composite matrix for cost reduction purpose.
- Development of partition panel boards and ceiling sheets using fabric-cement composite with improved thermal comfortability and acoustic performance.

References

- [1] C. P. Steve Evans, "Trans Textile Project Report," Center for Industrial Sustainability, United Kingdom, 2017.
- [2] N. A. J. H. M. Senthilkumar, "Elastane fabrics – A tool for stretch applications in sports," *Indian Journal of Fibre & Textile Research*, vol. 36, pp. 300-307, 2011.
- [3] U. C. Shuvo Kumar Kundu, "Effect of Fiber Content on Comfort Properties of Cotton/Spandex, Rayon/Spandex, and Polyester/Spandex Single Jersey Knitted Fabrics," *SSRG International journal of polymer and textile engineering*, vol. 5, no. 3, pp. 33-39, 2018.
- [4] B. P. Corbman, *Fiber to Fabric*, Gregg Division McGraw-Hill, 1983.
- [5] K. Singha, "Analysis of Spandex/Cotton Elastomeric Properties: Spinning and Applications," *International Journal of Composite Materials*, vol. 2, pp. 11-16, 2012.
- [6] J. Jerde, *Encyclopedia of Textiles*, Facts on File, 1992.
- [7] M. J. Aspiras F.F, "Utilization of Textile Waste Cuttings as Building Material," *Materials Processing Technology*, pp. 379-384, 1995.
- [8] U.D.G.U.C Udagama, A. K. Kulatunga, "Development of Sustainable Roofing material from Waste," 2014.
- [9] R. P. R. Selvaraj, "Study on Recycled Waste Cloth in Concrete," *International Journal of Engineering Research & Technology (IJERT)*, vol. 4, no. 9, pp. 891-895, 2015.
- [10] B. B. K. A. D. I.H. Jayasinghe, "Environmental Conservation Efforts in Developing Textile Waste Incorporated Cement Blocks," *Tropical Agricultural Research*, vol. 21, no. 2, pp. 126-133, 2010.
- [11] Saverio Spadea, Ilenia Farina, Anna Carrafiello, Fernando Fraternali, "Recycled nylon fibers as cement mortar reinforcement," *Construction and Building Materials*, pp. 200-209, 2015.
- [12] S. S. F. D. Alessandro P. Fantilli, "The use of wool as fiber-reinforcement in cement-based mortar," *Construction and Building Materials*, pp. 562-569, 2017.
- [13] F. D. S. S. F. Asdrubali, "A review of unconventional sustainable building insulation materials," *Sustainable Materials and Technologies*, vol. 4, pp. 1-17, 2015.
- [14] ISO_1833-1, "Textiles- Quantitative chemical analysis, Part-1: General principles of testing," International Standards Institution, 2006.

- [15] B. 1998, "Textiles- Fabrics- Determination of mass per unit area using small samples," British Standards Institution, 1998.
- [16] SLS_1144:Part-2, "Specification for ready mixed concrete, Part 2- Test methods," Sri Lanka Standards Institution, 1996.
- [17] BS812_PART-103.1, "Testing aggregates, Part 103.1- Methods for determination of particle size distribution- sieve tests," British Standards Institution, 1985.
- [18] BS812-Part2, "Sampling and testing of mineral aggregates, sands and fillers, Part 2- Physical properties," British standards Institution, 1975.
- [19] SLS_ISO_679, "Test methos for cements- Determination of strength," Sri Lanka Standards Institution, 2011.
- [20] SLS1425:Part-2, "Secification for concrete paving blocks, Part 2- Test methods," Sri Lanka Standards Institution, 2011.
- [21] BSEN1338:2003, "Concrete paving blocks- Rquirements and test methods," British Standards Institution, 2003.
- [22] N. H. A. Halim, "Permeability and Strength of Porous Concrete Paving Blocks at Different Sizes Coarse Aggrege," *Journal of Phsics*, vol. 1049, 2017.
- [23] BSEN_14808, "Surfaces for sports areas - Determination of shock absorption," British Standards Institution, 2005.
- [24] P. W. Elliott, "The physics of sports surface testing - Force reduction," ASET Services Publication, 2017.
- [25] ISO_8336, "Fiber cement flat sheets- Product specification and test methods," International Standards Organization, 2009.
- [26] BS882, "Specification for aggregates from natural sources for concrete," British Standards Institution, 1992.
- [27] SLS1425:Part1, "Specification for concrete paving blocks, Part 1: Requirements," Sri Lanka Standards Institution, 2011.
- [28] J. R. I. Z. Colin McPhee, "Relative Permeability," *Developments in peroleum Science*, vol. 64, pp. 519-653, 2015.
- [29] BSEN15330-1, "Surfaces for sports areas - Synthetic turf and needle punched surfaces primarily designed for outdoor use; Part 1- Specification for synthetic turf surfaces for football, hockey, rugby union training, tennis and multi-sports use," British Standards Institution, 2013.

- [30] "Play on courts," The Recreational Group, 2020. [Online]. Available: <https://www.playoncourts.com/wood-courts.html>. [Accessed 12 February 2020].
- [31] L. M. H. L. C. P. d. S. F. G. B. Â. S. P. Alexandre Lorenzi, "Thermal profiles in pervious concrete during summer rain simulations," *REVISTAMATERIA*, vol. 23, 2018.
- [32] J. W. T. N. M. I. T.C. Yang, "Methodology of accelerated weathering test through physicochemical analysis for polymeric materials in building construction," *Materials Research Innovation*, vol. 18, pp. 91-95, 2014.
- [33] D. Florence, "UV Inhibitors in Polyester Gelcoats," PCI paint and coating industry, 2002.